

# Power corrections to the space-like transition form factor

$$F_{\eta' g^* g^*}(Q^2, \omega, \eta)$$

S. S. Agaev\*

*The Abdus Salam International Centre for Theoretical Physics, I-34014 Trieste, Italy*

N. G. Stefanis†

*Institut für Theoretische Physik II,  
Ruhr-Universität Bochum, D-44780 Bochum, Germany*

(Dated: May 21, 2019)

## Abstract

Employing the standard hard-scattering approach (HSA) in conjunction with the running-coupling (RC) method, the latter joined with the infrared-renormalon calculus, we compute power-suppressed corrections  $\sim 1/Q^{2n}$ ,  $n = 1, 2, \dots$  to the massless  $\eta'$  meson - virtual gluon transition form factor (FF)  $Q^2 F_{\eta' g^* g^*}(Q^2, \omega)$ . Contributions to the form factor from the quark and gluon components of the  $\eta'$  meson are taken into account. Analytic expressions for the FF's  $F_{\eta' gg^*}(Q^2, \omega = \pm 1)$  and  $F_{\eta' g^* g^*}(Q^2, \omega = 0)$  are also presented, as well as Borel transforms  $B[Q^2 F_{\eta' g^* g^*}](u)$  and resummed expressions. It is shown that except for  $\omega = \pm 1, 0$ , the Borel transform contains an infinite number of infrared renormalon poles. It is demonstrated that in the explored range of the total gluon virtuality  $1 \text{ GeV}^2 \leq Q^2 \leq 25 \text{ GeV}^2$ , power corrections found with the RC method considerably enhance the FF  $F_{\eta' g^* g^*}(Q^2, \omega)$  relative to results obtained only in the context of the standard HSA with a “frozen” coupling.

PACS numbers: 12.38.Bx, 11.10.Hi, 11.10.Jj, 14.40.Aq

---

\*Electronic address: agaev.shahin@yahoo.com; Permanent address: High Energy Physics Lab., Baku State University, Z. Khalilov St. 23, 370148 Baku, Azerbaijan

†Electronic address: stefanis@tp2.ruhr-uni-bochum.de

## I. INTRODUCTION

During the last few years the interest into theoretical investigations of the quark-gluon structure of light mesons, especially the pion,  $\eta$ , and  $\eta'$  mesons, has risen due to the high-precision CLEO results on the electromagnetic  $M\gamma$  transition form factors (FF's)  $F_{M\gamma}(Q^2)$  [1] (with  $M$  denoting one of these mesons), as well as because of the observed very large branching ratios for the exclusive  $B \rightarrow K\eta'$  and semi-inclusive  $B \rightarrow \eta'X_s$  decays [2].

The data on the  $\eta'\gamma$  transition FF were mainly used for extracting information concerning the  $\eta'$  quark component of the meson distribution amplitude (DA). Schemes and methods applied to this purpose range from light-cone perturbation-theory calculations – with the quark transverse-momentum  $k_\perp$  dependence kept in the hard-scattering amplitude  $T_H(x, k_\perp, Q^2)$  of the underlying hard subprocess [3] – to the modified hard-scattering approach (mHSA) with resummed transverse-momentum effects (giving rise to Sudakov suppression factors) and such due to the intrinsic transverse momentum of the meson wave functions [4, 5], to the running coupling (RC) method, employed for the estimation of power-suppressed corrections to the  $\eta'\gamma$  transition FF [6]. In these investigations, two different parameterizations were used, one employing the conventional  $\eta - \eta'$  mixing scheme with one mixing angle  $\theta_p$  [3, 4, 6] for both physical states and decay constants and a second one, which considers two mixing angles  $\theta_1$  and  $\theta_8$  to parameterize the weak decay constants  $f_P^i$  ( $P = \eta, \eta'$ ;  $i = 1, 8$ ) of the  $\eta$  and  $\eta'$  mesons [5]. An important conclusion drawn from these investigations, irrespective of the underlying method, is that the  $\eta'$ -meson DA must be close to its asymptotic form and that the admixture of the first non-asymptotic term should be within the range  $b_2(\mu_0^2) \simeq 0.05 \div 0.15$ ,  $b_2$  being the first Gegenbauer coefficient. The CLEO data on the  $\eta'\gamma$  transition and the two-angle mixing scheme were also used to estimate the allowed range of the intrinsic charm content of the  $\eta'$  meson decay constant  $f_{\eta'}^c$  [5]. It turned out that the value  $-65 \text{ MeV} \leq f_{\eta'}^c \leq 15 \text{ MeV}$  does not contradict the CLEO data.

But apart from the ordinary light quark and charm  $|\eta'_c\rangle$  components, the  $\eta'$  meson may also contain a two-gluon valence Fock state  $|gg\rangle$  as well. Moreover, absent at the normalization point  $\mu_0$ , a gluon component of the  $\eta'$  meson will appear in the region  $Q^2 > \mu_0^2$  owing to quark-gluon mixing and renormalization-group evolution of the  $\eta'$  meson DA [7, 8, 9, 10, 11]. This can directly contribute to the  $\eta'\gamma$  transition at the next-to-leading order due to quark box diagrams and also affect the leading-order result through evolution of the quark component of the  $\eta'$ -meson DA. Hence, an effect of the  $\eta'$  meson gluon component on the  $\eta'\gamma$  transition is only mild and was therefore neglected in most theoretical investigations [3, 4, 5, 6].

But the contribution of the gluon content of the  $\eta'$  meson to the two-body non-leptonic exclusive and semi-inclusive decay ratios of the  $B$  meson may be sizeable. Indeed, such a mechanism to account for the observed large branching ratio [2]

$$Br(B \rightarrow \eta' + X_s) = (6.2 \pm 1.6 \pm 1.3) \times 10^{-4}, \quad (1.1)$$

was proposed in Ref. [12]. In this work it was suggested that the dominant fraction of the  $B \rightarrow \eta' + X_s$  decay rate appears as the result of the transition  $g^* \rightarrow g\eta$  of a virtual gluon  $g^*$  from the standard model penguin  $b \rightarrow sg^*$ . For the computation of the contribution of this mechanism to the  $Br(B \rightarrow \eta' + X_s)$  in Ref. [12], the  $g^*g\eta'$  vertex function was approximated by the constant  $H(q^2, 0, m_{\eta'}^2) \simeq H(0, 0, m_{\eta'}^2) \simeq 1.8 \text{ GeV}^{-1}$ , the latter being extracted from the analysis of the  $J/\psi \rightarrow \eta'\gamma$  decay. Further investigations, however, demonstrated that effects of the QCD running coupling  $\alpha_s(q^2)$  [13], as well as a momentum dependence of the

form factor  $H(q^2, 0, m_{\eta'}^2)$ , properly taken into account, considerably reduce the contribution to Eq. (1.1) of the mechanism under consideration [14]. In order to cover a gap between theoretical predictions and experimental data in Ref. [15], a gluon fusion mechanism was proposed. In accordance with the latter, the  $\eta'$  meson is produced by the fusion of a gluon from the QCD penguin diagram  $b \rightarrow sg^*$  with another one emitted by the light quark inside the  $B$  meson. In this mechanism, the form factor <sup>1</sup>  $F_{\eta'g^*g^*}(q_1^2, q_2^2, m_{\eta'}^2)$  appears owing to the  $g^*g^* \rightarrow \eta'$  transition.

The same ideas form a basis for the computation of the branching ratios of various two-body non-leptonic exclusive decay modes of the  $B$  meson [16]. To account for the data on the exclusive decay  $B \rightarrow K\eta'$  in Ref. [17], a mechanism was proposed, based on the assumption of a strong intrinsic charm component of the  $\eta'$  meson. But a more detailed analysis [18] proved that the charm content of the  $\eta'$  is too small ( $f_{\eta'}^c \simeq -2$  MeV) to explain the observed branching ratio  $Br(B \rightarrow K\eta')$ . The CLEO data on the  $B$  meson non-leptonic decays that stimulated interesting theoretical works [19] remain actual until today [20].

The  $\eta'$  meson - virtual (on-shell) gluon transition form factor  $F_{\eta'g^*g^*}(q_1^2, q_2^2, m_{\eta'}^2)$  is the central ingredient of performed analyses and hence requires further thorough investigations within perturbative QCD (PQCD). Calculations of this FF within PQCD were performed in [21, 22, 23, 24]. In Ref. [21] the contribution of the gluon content of the  $\eta'$  meson to the form factor  $F_{\eta'gg^*}(q_1^2, 0, m_{\eta'}^2)$  was estimated and found to be too small, while  $F_{\eta'gg^*}(q_1^2, 0, m_{\eta'}^2)$  itself is close to the form

$$F_{\eta'gg^*}(q_1^2, 0, m_{\eta'}^2) \simeq \frac{H(0, 0, m_{\eta'}^2)}{q_1^2/m_{\eta'}^2 - 1} = \frac{1.8}{q_1^2/m_{\eta'}^2 - 1} \text{ GeV}^{-1}, \quad (1.2)$$

used in some phenomenological applications [14, 15]. In computations of the  $\eta'$  meson - virtual gluon vertex function  $F_{\eta'g^*g^*}(q_1^2, q_2^2, m_{\eta'}^2)$ , the gluon content of the  $\eta'$  meson was neglected and the asymptotic form of the DA for the quark component was employed [22]. The same vertex function  $F_{\eta'g^*g^*}(q_1^2, q_2^2, m_{\eta'}^2)$  was considered in [23], where the standard HSA [25], as well as the mHSA were used and the space-, and time-like vertex functions were analyzed. In Ref. [24], the space-like form factor  $F_{\eta'g^*g^*}(Q^2, \omega)$  was computed within the standard HSA. In this work, a detailed analysis of the normalization of the gluon component of the  $\eta'$ -meson DA and that of the gluon projector onto a pseudoscalar meson state was presented.

In the present work we investigate the  $\eta'$  meson - virtual gluon space-like transition form factor  $F_{\eta'g^*g^*}(Q^2, \omega)$  in the framework of the standard HSA [25], as well as by applying the RC method together with the infrared (IR) renormalon calculus [26]. Our central aim is the calculation and evolution of power-suppressed corrections  $\sim 1/Q^{2n}$ ,  $n = 1, 2, \dots$  to the transition FF  $Q^2 F_{\eta'g^*g^*}(Q^2, \omega)$ . Because in the production of the  $\eta'$  meson from the  $B$  decay the momentum squared of the virtual gluon can vary from  $1$  GeV $^2$  to  $25$  GeV $^2$ , the power corrections in this domain of  $Q^2$  should play an important role.

The RC method enables us to estimate power corrections coming from the end-point  $x, y \rightarrow 0, 1$  regions (for definiteness we consider two mesons in an exclusive process) in the integrals determining the amplitude for an exclusive process. It is known [25] that in order to calculate an amplitude of some hadron exclusive process, one has to perform integrations over longitudinal momentum fractions  $x, y$  of the involved partons. If one chooses the

---

<sup>1</sup> In this work we use the notions “vertex function” and “form factor” on the same footing.

renormalization scale  $\mu_R^2$  in the hard-scattering amplitude  $T_H$  of the corresponding partonic subprocess in such a way as to minimize higher-order corrections and allows the QCD coupling constant  $\alpha_s(\mu_R^2)$  to run, then one encounters divergences arising from the end-point  $x, y \rightarrow 0, 1$  regions. The reason is that the scale  $\mu_R^2$ , as a rule, is equal to the momentum squared of the hard virtual partons, the latter carrying the strong interactions in the subprocess' Feynman diagrams [27] and, in general, depends on  $x$  and  $y$ . Within the RC method this problem is resolved by applying the IR renormalon calculus. It turns out that this treatment allows us to evaluate power-behaved corrections to the physical quantity under investigation. This method was recently used for the computation of power corrections to the electromagnetic form factors  $F_{\pi,K}(Q^2)$  of the pion and the kaon, [28, 29], and the electromagnetic transition FF's  $F_{M\gamma}(Q^2)$  [6, 30] of the light pseudoscalar mesons. Power corrections to hadronic processes can also be calculated utilizing the Landau-pole free expression for the QCD coupling constant [31]. This analytic approach was used to compute in a unifying way power corrections to the electromagnetic pion form factor and to the inclusive cross section of the Drell-Yan process [32, 33]. Such an investigation of the processes considered in this work is in progress.

The paper is organized as follows. In Sect. II we consider various  $\eta - \eta'$  mixing schemes in the flavor  $SU_f(3)$  octet-singlet and quark-flavor bases and the evolution of the quark and gluon components of the  $\eta'$  meson DA with the factorization scale. The important question of the generalization of the hard-scattering amplitudes of the  $\eta'g^*$  transition to the RC method case is also considered. Section III is devoted to a rather detailed presentation of the RC method. In Sect. IV we compute the quark and gluon components of the transition FF  $F_{\eta'g^*g^*}(Q^2, \omega)$ . Section V contains our numerical results. Finally, in Sect. VI we make our concluding remarks.

## II. QUARK AND GLUON CONTRIBUTIONS TO THE $\eta' - g^*$ TRANSITION FORM FACTOR

In this section we consider the quark-gluon content of the  $\eta'$  meson, as well as the  $\eta'$  DA and give some general expressions for determining the  $\eta'g^*$  transition form factor within both the standard HSA and the RC method.

### A. Structure of the $\eta'$ meson

The parton Fock state decomposition of the pseudoscalar  $P = \eta, \eta'$  mesons, can be generically presented in the following form

$$|P\rangle = |P_a\rangle + |P_b\rangle + |P_c\rangle + |P_g\rangle, \quad (2.1)$$

where  $|P_a\rangle$  and  $|P_b\rangle$  denote the  $P$ -meson light-quarks  $u, d, s$  and  $|P_c\rangle, |P_g\rangle$  its charm and gluon components, respectively. Fock states with additional gluons and  $q\bar{q}$  quark-antiquark pairs have been omitted for simplicity.

The  $P$ -meson light-quark content  $|P_a\rangle, |P_b\rangle$  can be described either in the flavor  $SU_f(3)$  octet-singlet or in the quark-flavor basis. In the first scheme,  $|P_a\rangle, |P_b\rangle$  are expressed as superpositions of the  $SU_f(3)$  octet  $\eta_8$  and singlet  $\eta_1$  states

$$|\eta_1\rangle = \frac{\Psi_1}{\sqrt{3}} |u\bar{u} + d\bar{d} + s\bar{s}\rangle,$$

$$|\eta_8\rangle = \frac{\Psi_8}{\sqrt{6}} |u\bar{u} + d\bar{d} - 2s\bar{s}\rangle, \quad (2.2)$$

whereas in the quark-flavor basis, the  $SU_f(3)$  strange  $\eta_s$  and non-strange  $\eta_q$  states are used, i.e.,

$$|\eta_q\rangle = \frac{\Psi_q}{\sqrt{2}} |u\bar{u} + d\bar{d}\rangle, \quad |\eta_s\rangle = \Psi_s |s\bar{s}\rangle. \quad (2.3)$$

In Eqs. (2.2) and (2.3)  $\Psi_i$  denote wave functions of the corresponding parton states.

As mentioned above, the charm component of the  $\eta'$  meson was estimated [18, 34] to be too small to considerably affect the  $B$  meson exclusive decays. Therefore, in the present investigation we neglect the charm content of the  $\eta'$  meson. On the other hand, the admixture of the gluon component

$$|\eta'_g\rangle \sim \Psi_g |\eta_g\rangle = \Psi_g |gg\rangle,$$

with the light-quark content can be described in the quark-flavor basis employing the parameterization [35]

$$|\eta'\rangle = X_{\eta'} |\eta_q\rangle + Y_{\eta'} |\eta_s\rangle + Z_{\eta'} |\eta_g\rangle, \quad (2.4)$$

where the constants  $X_{\eta'}$ ,  $Y_{\eta'}$  and  $Z_{\eta'}$  are normalized according to

$$X_{\eta'}^2 + Y_{\eta'}^2 + Z_{\eta'}^2 = 1.$$

The phenomenological analysis performed in Ref. [36] led to the conclusion that the maximal admixture of the two-gluon state in the  $\eta'$  meson does not exceed 26%, the percentage being computed with the aid of the formula

$$R = \frac{Z_{\eta'}}{X_{\eta'} + Y_{\eta'} + Z_{\eta'}}.$$

Recently, the KLOE Collaboration reported a measurement of the mixing angle  $\phi_p$  of the  $\eta, \eta'$  mesons in the quark-flavor basis [37]. In this latter work, the coefficient  $Z_{\eta'}$  was estimated to be

$$Z_{\eta'}^2 = 0.06^{+0.09}_{-0.06},$$

a value consistent with a  $|\eta'_g\rangle$  fraction below 15%.

The pure light-quark sector of the  $\eta - \eta'$  system without charm and gluon admixtures can be treated by means of the basic states (2.2) and (2.3). In the  $SU_f(3)$  octet-singlet basis, the  $\eta$  and  $\eta'$  mesons are expressed as superpositions of the  $\eta_8$ ,  $\eta_1$  states

$$\begin{aligned} |\eta\rangle &= \cos \theta_p |\eta_8\rangle - \sin \theta_p |\eta_1\rangle, \\ |\eta'\rangle &= \sin \theta_p |\eta_8\rangle + \cos \theta_p |\eta_1\rangle. \end{aligned} \quad (2.5)$$

Here,  $\theta_p$  is the mixing angle of physical states in the octet-singlet scheme. In the quark-flavor basis we get the same expressions but with  $\theta_p$  replaced by the mixing angle  $\phi_p$  of the physical states in the new basis  $\eta_q$ ,  $\eta_s$ , viz.,

$$\begin{aligned} |\eta\rangle &= \cos \phi_p |\eta_q\rangle - \sin \phi_p |\eta_s\rangle, \\ |\eta'\rangle &= \sin \phi_p |\eta_q\rangle + \cos \phi_p |\eta_s\rangle. \end{aligned} \quad (2.6)$$

The  $\eta_1$  and  $\eta_8$  states and the mixing angle  $\theta_p$  in the octet-singlet scheme can be expressed in terms of the  $\eta_q$ ,  $\eta_s$  states and the mixing angle  $\phi_p$  in the quark-flavor basis and vice versa. Notably, if one starts from the quark-flavor basis (2.3), assuming that the orthogonal  $\eta_q$  and  $\eta_s$  states are pure ones, i.e., do not contain  $s\bar{s}$  and  $u\bar{u}$ ,  $d\bar{d}$  admixtures, then one may perform a rotation with the ideal mixing angle to obtain Eq. (2.5) from Eq. (2.6) with  $\theta_p = \phi_p - \arctan \sqrt{2}$ . But due to the flavor  $SU_f(3)$  symmetry-breaking effects, the  $\eta_1$  and  $\eta_8$  states contain  $SU_f(3)$  octet  $\eta_8$  and singlet  $\eta_1$  admixtures and Eq. (2.2) holds only in the flavor-symmetry limit  $\Psi_s = \Psi_q$  [38]. Alternatively, one can start from the assumption that the  $\eta_1$  and  $\eta_8$  states defined in Eq. (2.2) have no  $\eta_8$  and  $\eta_1$  admixtures and then rotate these states back by the ideal mixing angle to get Eq. (2.6) from Eq. (2.5), but now with  $\eta_q$  and  $\eta_s$  states containing  $s\bar{s}$  and  $u\bar{u}$ ,  $d\bar{d}$  components, which break Eq. (2.3).

As seen at the level of physical-state mixing, there is no difference between the two bases (2.2) and (2.3). This only appears when one parameterizes the decay constants  $f_P^i$  of the  $P = \eta$  and  $\eta'$  mesons in terms of

$$\langle 0 | J_{\mu 5}^i | P \rangle = i f_P^i p_\mu,$$

where  $J_{\mu 5}^i$  is the axial-vector currents with  $i = q, s$  or  $i = 1, 8$ . In the quark-flavor basis the decay constants  $f_P^{q(s)}$  follow with great accuracy the pattern of the state mixing [38, 39]

$$\begin{aligned} f_\eta^q &= f_q \cos \phi_p, & f_\eta^s &= -f_s \sin \phi_p, \\ f_{\eta'}^q &= f_q \sin \phi_p, & f_{\eta'}^s &= f_s \cos \phi_p. \end{aligned} \quad (2.7)$$

In order to take into account the flavor symmetry breaking effects in the octet-singlet basis, the two mixing-angles scheme for the decay constants  $f_P^{1(8)}$  was introduced [40]

$$\begin{aligned} f_\eta^8 &= f_8 \cos \theta_8, & f_\eta^1 &= -f_1 \sin \theta_1, \\ f_{\eta'}^8 &= f_8 \sin \theta_8, & f_{\eta'}^1 &= f_1 \cos \theta_1. \end{aligned} \quad (2.8)$$

The mixing angles  $\theta_1$  and  $\theta_8$  differ from each other and also from the state mixing angle  $\theta_p$ . In the conventional octet-singlet mixing scheme, one supposes that the decay constants  $f_P^{1(8)}$  follow the pattern of the physical state mixing (2.5) and  $\theta_1 = \theta_8 = \theta_p$ . In phenomenological applications, both the octet-mixing and quark-flavor bases may be used. A detailed analysis of the  $\eta - \eta'$  mixing problems and further references can be found in Ref. [41].

In our present work we choose the quark-flavor basis (2.3) and the mixing scheme (2.6). In this scheme, the decay constants  $f_q$  and  $f_s$  and the mixing angle  $\phi_p$  have the following values [39, 41]

$$f_q = (1.07 \pm 0.02) f_\pi, \quad f_s = (1.34 \pm 0.06) f_\pi, \quad \phi_p = 39.3^\circ \pm 1.0^\circ,$$

with  $f_\pi = 0.131 \text{ GeV}$  being the pion weak decay constant. The KLOE result for  $\phi_p = (41.8^\circ \pm 1.6^\circ)$  [34] is slightly shifted towards larger values, but still does not contradict the average value  $\phi_p = 39.3^\circ \pm 1.0^\circ$ . In our numerical computations we shall use the central values of the constants shown above.

The  $\eta'$  meson DA  $\phi(x, \mu^2)$  obtained by solving the evolution equation [9, 10, 11] is given by the expression

$$\phi(x, \mu^2) = \phi^q(x, \mu^2) + \phi^g(x, \mu^2), \quad (2.9)$$

where the functions  $\phi^q(x, \mu^2)$  and  $\phi^g(x, \mu^2)$  denote, respectively, the quark and gluon components of the  $\eta'$  meson DA. They satisfy the symmetry and antisymmetry conditions,

$$\phi^q(x, \mu^2) = \phi^q(1 - x, \mu^2), \quad \phi^g(x, \mu^2) = -\phi^g(1 - x, \mu^2). \quad (2.10)$$

This follows from the symmetry properties of the DA of the two-particle bound state of a neutral pseudoscalar meson and is in fact enough to obtain general expressions for the  $\eta'$  meson - virtual gluon transition form factor. The evolution of the functions  $\phi^q(x, \mu^2)$  and  $\phi^g(x, \mu^2)$  with the scale  $\mu^2$ , as well as their dependence on the constants  $f_q$ ,  $f_s$  and  $\phi_p$  will be considered in Subsect. II.3.

### B. The $\eta' - g^*$ transition form factor $F_{\eta' g^* g^*}(\mathbf{Q}^2, \omega)$

The  $\eta'$  meson - virtual gluon transition form factor  $F_{\eta' g^* g^*}(Q^2, \omega)$

$$F_{\eta' g^* g^*}(Q^2, \omega) = F_{\eta' g^* g^*}^q(Q^2, \omega) + F_{\eta' g^* g^*}^g(Q^2, \omega), \quad (2.11)$$

can be defined in terms of the invariant amplitude

$$M = M^q + M^g, \quad (2.12)$$

for the process

$$\eta'(P) \rightarrow g^*(q_1) + g^*(q_2), \quad (2.13)$$

in the following way

$$M^{q(g)} = -i F_{\eta' g^* g^*}^{q(g)}(Q^2, \omega) \delta_{ab} \epsilon^{\mu\nu\rho\sigma} \epsilon_\mu^{a*} \epsilon_\nu^{b*} q_{1\rho} q_{2\sigma}. \quad (2.14)$$

In Eq. (2.14)  $\epsilon_\mu^a$ ,  $\epsilon_\nu^b$  and  $q_1$ ,  $q_2$  are, respectively, the polarization vectors and four-momenta of the two gluons. Because we study only the space-like FF,  $q_1^2$  and  $q_2^2$  obey the constraints  $Q_1^2 = -q_1^2 \geq 0$ ,  $Q_2^2 = -q_2^2 > 0$  and  $Q_1^2 = -q_1^2 > 0$ ,  $Q_2^2 = -q_2^2 \geq 0$ . The form factor  $F_{\eta' g^* g^*}(Q^2, \omega)$  depends on the total gluon virtuality  $Q^2$  and the asymmetry parameter  $\omega$ , defined by

$$Q^2 = Q_1^2 + Q_2^2, \quad \omega = \frac{Q_1^2 - Q_2^2}{Q^2}. \quad (2.15)$$

The asymmetry parameter  $\omega$  varies in the region  $-1 \leq \omega \leq 1$ . The value  $\omega = \pm 1$  corresponds to the  $\eta'$  meson - on-shell gluon transition and  $\omega = 0$  to the situation when the gluons have equal virtualities  $Q_1^2 = Q_2^2$ .

In accordance with the factorization theorems of PQCD at high momentum transfer, the FF's  $F_{\eta' g^* g^*}^{q(g)}(Q^2, \omega)$  are given by the expressions

$$F_{\eta' g^* g^*}^q(Q^2, \omega) = [T_H^q(x, Q^2, \omega, \mu_F^2) + T_H^q(\bar{x}, Q^2, \omega, \mu_F^2)] \otimes \phi^q(x, \mu_F^2), \quad (2.16)$$

and

$$F_{\eta' g^* g^*}^g(Q^2, \omega) = [T_H^g(x, Q^2, \omega, \mu_F^2) - T_H^g(\bar{x}, Q^2, \omega, \mu_F^2)] \otimes \phi^g(x, \mu_F^2). \quad (2.17)$$

Here,  $\bar{x} \equiv 1 - x$ , and  $\mu_F^2$  represents the factorization scale. In Eqs. (2.16) and (2.17) we have used the notation

$$T_H(x, Q^2, \omega, \mu_F^2) \otimes \phi(x, \mu_F^2) = \int_0^1 T_H(x, Q^2, \omega, \mu_F^2) \phi(x, \mu_F^2) dx. \quad (2.18)$$

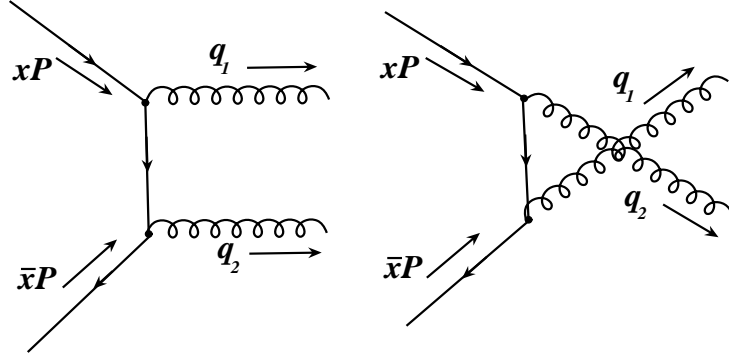


FIG. 1: Leading order Feynman diagrams contributing to the hard-scattering subprocess  $q + \bar{q} \rightarrow g^* + g^*$ .

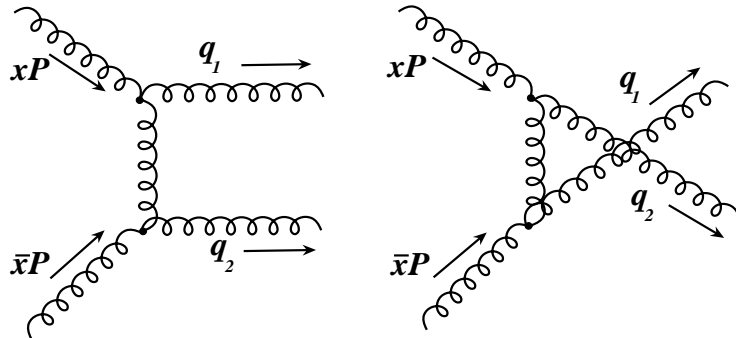


FIG. 2: Feynman diagrams contributing at leading order to the subprocess  $g + g \rightarrow g^* + g^*$ .

The sum

$$T_H^q(x, Q^2, \omega, \mu_F^2) + T_H^q(\bar{x}, Q^2, \omega, \mu_F^2), \quad (2.19)$$

and the difference

$$T_H^g(x, Q^2, \omega, \mu_F^2) - T_H^g(\bar{x}, Q^2, \omega, \mu_F^2), \quad (2.20)$$

represent the hard-scattering amplitudes of the subprocesses  $q + \bar{q} \rightarrow g^* + g^*$  and  $g + g \rightarrow g^* + g^*$ , respectively. The Feynman diagrams contributing at the leading order to these subprocesses' amplitudes are depicted in Figs. 1 and 2.

In what follows, we omit the subscript  $H$  in Eqs. (2.19) and (2.20) and introduce instead the notations

$$T_1^{q(g)}(x, Q^2, \omega, \mu_F^2) = T_H^{q(g)}(x, Q^2, \omega, \mu_F^2),$$

$$T_2^{q(g)}(x, Q^2, \omega, \mu_F^2) = T_H^{q(g)}(\bar{x}, Q^2, \omega, \mu_F^2).$$

For the hard-scattering amplitudes  $T_1^{q(g)}$  and  $T_2^{q(g)}$  at leading order of PQCD we get

$$\begin{aligned} T_1^q(x, Q^2, \omega, \mu_R^2) &= -\frac{4\pi}{3Q^2} \frac{\alpha_s(\mu_R^2)}{(1+\omega)x + (1-\omega)\bar{x}}, \\ T_2^q(x, Q^2, \omega, \bar{\mu}_R^2) &= -\frac{4\pi}{3Q^2} \frac{\alpha_s(\bar{\mu}_R^2)}{(1+\omega)\bar{x} + (1-\omega)x} \end{aligned} \quad (2.21)$$

and

$$\begin{aligned} T_1^g(x, Q^2, \omega, \mu_R^2) &= \frac{\pi\alpha_s(\mu_R^2)}{Q^2 n_f} \frac{(1+\omega)x + (1-\omega)\bar{x}}{\omega[(1+\omega)\bar{x} + (1-\omega)x]}, \\ T_2^g(x, Q^2, \omega, \bar{\mu}_R^2) &= \frac{\pi\alpha_s(\bar{\mu}_R^2)}{Q^2 n_f} \frac{(1+\omega)\bar{x} + (1-\omega)x}{\omega[(1+\omega)x + (1-\omega)\bar{x}]} \end{aligned} \quad (2.22)$$

(Note that in the limit  $\omega = 0$  the difference  $T_1^g - T_2^g$ , being the physical hard-scattering amplitude, is singularity-free - see Eq. (4.27) below.) Here,  $\alpha_s(\mu^2)$  is the QCD coupling constant in two-loop approximation defined by

$$\alpha_s(\mu^2) = \frac{4\pi}{\beta_0 \ln(\mu^2/\Lambda^2)} \left[ 1 - \frac{2\beta_1}{\beta_0^2} \frac{\ln \ln(\mu^2/\Lambda^2)}{\ln(\mu^2/\Lambda^2)} \right], \quad (2.23)$$

with  $\beta_0$  and  $\beta_1$  being the one- and two-loop coefficients of the QCD beta function:

$$\beta_0 = 11 - \frac{2}{3}n_f, \quad \beta_1 = 51 - \frac{19}{3}n_f. \quad (2.24)$$

In Eqs. (2.22), (2.23) and (2.24)  $\Lambda = 0.3$  GeV is the QCD scale parameter and  $n_f = 3$  is the number of active quark flavors.

The physical quantity  $F_{\eta'g^*g^*}(Q^2, \omega)$ , represented at sufficiently high  $Q^2$  by the factorization formulas (2.16), (2.17) is independent of the renormalization scheme and the renormalization and factorization scales  $\mu_R^2$  ( $\bar{\mu}_R^2$ ) and  $\mu_F^2$ . Truncation of the perturbation series of  $F_{\eta'g^*g^*}(Q^2, \omega)$  at any finite order causes a residual dependence on the scheme as well as on these scales. At the leading order of PQCD, the hard-scattering amplitude does not depend on the factorization scale  $\mu_F^2$  but depends implicitly on the renormalization scale  $\mu_R^2$  through  $\alpha_s(\mu_R^2)$ .<sup>2</sup> An explicit dependence of the function  $T_H$  on  $\mu_R^2$  and  $\mu_F^2$  appears at  $O(\alpha_s)$  due to QCD corrections. As the scales  $\mu_R^2$  and  $\mu_F^2$  are independent of each other and can be chosen separately, we adopt in this work the natural and widely used “default” choice for the factorization scale  $\mu_F^2 = Q^2$  and omit in what follows a dependence of the hard-scattering amplitude on  $\mu_F^2$  (see, Eqs. (2.21) and (2.22)). For a more detailed discussion of these questions, we refer the interested reader to [42].

In the standard HSA with a “frozen” coupling constant [25] one sets the renormalization scale to be  $\mu_R^2 = \bar{\mu}_R^2 = Q^2$ , simplifying the calculation of the vertex function  $F_{\eta'g^*g^*}(Q^2, \omega)$  considerably. In this approach the hard-scattering amplitudes  $T_{1,2}^{q(g)}$  and hence the quark and

---

<sup>2</sup> Similar arguments hold for the scale  $\bar{\mu}_R^2$ .

gluon components of the vertex function  $F_{\eta'g^*g^*}(Q^2, \omega)$  possess symmetry features pertaining to the RC method. Indeed, it is not difficult to see that

$$T_{1(2)}^q(\bar{x}, Q^2, \omega) = T_{2(1)}^q(x, Q^2, \omega), \quad T_{1(2)}^q(x, Q^2, -\omega) = T_{2(1)}^q(x, Q^2, \omega), \quad (2.25)$$

and

$$T_{1(2)}^g(\bar{x}, Q^2, \omega) = T_{2(1)}^g(x, Q^2, \omega), \quad T_{1(2)}^g(x, Q^2, -\omega) = -T_{2(1)}^g(x, Q^2, \omega). \quad (2.26)$$

Using Eqs. (2.10) and (2.25), we then find

$$\begin{aligned} F_{\eta'g^*g^*}^q(Q^2, \omega) &= T_1^q(x, Q^2, \omega) \otimes \phi^q(x, Q^2) + T_2^q(x, Q^2, \omega) \otimes \phi^q(x, Q^2) \\ &= T_1^q(x, Q^2, \omega) \otimes \phi^q(x, Q^2) + T_1^q(x, Q^2, -\omega) \otimes \phi^q(x, Q^2) \\ &= T_1^q(x, Q^2, \omega) \otimes \phi^q(x, Q^2) + (\omega \leftrightarrow -\omega). \end{aligned} \quad (2.27)$$

At the same time

$$\begin{aligned} F_{\eta'g^*g^*}^q(Q^2, \omega) &= T_1^q(x, Q^2, \omega) \otimes \phi^q(x, Q^2) + T_1^q(\bar{x}, Q^2, \omega) \otimes \phi^q(x, Q^2) \\ &= T_1^q(x, Q^2, \omega) \otimes \phi^q(x, Q^2) + T_1^q(x, Q^2, \omega) \otimes \phi^q(\bar{x}, Q^2) \\ &= 2T_1^q(x, Q^2, \omega) \otimes \phi^q(x, Q^2) \end{aligned} \quad (2.28)$$

and

$$F_{\eta'g^*g^*}^q(Q^2, \omega) = 2T_2^q(x, Q^2, \omega) \otimes \phi^q(x, Q^2).$$

In similar manner, using Eqs. (2.10) and (2.26), one can demonstrate that the following equalities hold

$$\begin{aligned} F_{\eta'g^*g^*}^g(Q^2, \omega) &= T_1^g(x, Q^2, \omega) \otimes \phi^g(x, Q^2) - T_2^g(x, Q^2, \omega) \otimes \phi^g(x, Q^2) \\ &= T_1^g(x, Q^2, \omega) \otimes \phi^g(x, Q^2) + (\omega \leftrightarrow -\omega) \end{aligned} \quad (2.29)$$

and

$$F_{\eta'g^*g^*}^g(Q^2, \omega) = 2T_1^g(x, Q^2, \omega) \otimes \phi^g(x, Q^2) = -2T_2^g(x, Q^2, \omega) \otimes \phi^g(x, Q^2). \quad (2.30)$$

From Eqs. (2.27) and (2.29) it follows that

$$F_{\eta'g^*g^*}^q(Q^2, \omega) = F_{\eta'g^*g^*}^q(Q^2, -\omega), \quad F_{\eta'g^*g^*}^g(Q^2, \omega) = F_{\eta'g^*g^*}^g(Q^2, -\omega). \quad (2.31)$$

In PQCD calculations higher-order corrections to various physical processes, are, in general, large and in order to improve the convergence of the corresponding perturbative series, different methods have been proposed. In exclusive processes - considering the pion electromagnetic form factor as being a prominent example - the next-to-leading order  $O(\alpha_s)$  correction contains logarithmic terms  $\sim \ln(Q^2 \bar{x} \bar{y} / \mu_R^2)$  (or  $\sim \ln(Q^2 x y / \mu_R^2)$ ) [43, 44], which

can be entirely or partly eliminated by a proper choice of the renormalization scale  $\mu_R^2$  ( $\overline{\mu}_R^2$ ). This can be achieved by taking as a renormalization scale  $\mu_R^2 = Q^2\overline{xy}$  [ $\overline{\mu}_R^2 = Q^2xy$ ] or  $\mu_R^2 = Q^2\overline{x}/2$  [ $\overline{\mu}_R^2 = Q^2x/2$ ]. The renormalization scale enters into the PQCD expression not only via logarithmic terms, but also through the argument of the running coupling  $\alpha_s(\mu_R^2)$ . In order to calculate the amplitude of an exclusive process, an integration in corresponding integrals over the longitudinal momentum fractions of the quarks and gluons in the involved hadrons has to be carried out. Thus, in the pion electromagnetic FF calculations, the integration over the variables  $x$  and  $y$  has to be performed. Traditionally, to avoid problems associated with singularities of  $\alpha_s(\mu_R^2)$ , one “freezes” the running coupling by replacing  $x$  and  $y$ , e.g., by their mean values  $x \rightarrow \langle x \rangle = 1/2$ ,  $y \rightarrow \langle y \rangle = 1/2$  in the argument of  $\alpha_s(\mu_R^2)$  and performs then the calculation with  $\alpha_s(Q^2/4)$  [43]. Recently, the RC method for the calculation of various exclusive processes with  $\alpha_s(\mu_R^2)$  was proposed. Within this framework, one expresses the running coupling  $\alpha_s(\lambda Q^2)$  in terms of  $\alpha_s(Q^2)$  by employing the renormalization-group equation and performs the integration over  $x$  ( $y$ ) using the principal value prescription. It turns out that such an integration allows one to estimate power-suppressed corrections to the process under consideration, which improve the agreement of QCD theoretical predictions with experimental data. An alternative option would be to use the analytic perturbation theory [31] along the lines proposed in [32, 33]. Next-to-leading order corrections are known for only a few exclusive processes [43, 44, 45]. In general, the renormalization scale  $\mu_R^2$  may be taken equal or proportional to the square of the four-momentum  $q^2$  of the virtual parton(s) mediating the strong interaction in corresponding leading-order Feynman diagrams. In some cases, when  $q^2$  depends on other parameters of the process, like the asymmetry parameter  $\omega$  as in the case of  $F_{\eta'g^*g^*}(Q^2, \omega)$ , the renormalization scale  $\mu_R^2$  may be set equal to a fraction of  $q^2 \sim Q^2x$ .

In order to estimate power-suppressed corrections to the vertex function  $F_{\eta'g^*g^*}(Q^2, \omega)$  we adopt in this work the choice

$$\mu_R^2 = Q^2x, \quad \overline{\mu}_R^2 = Q^2\overline{x}, \quad (2.32)$$

which, in the  $\eta'$  meson - on-shell gluon transition, becomes equal to  $|q^2|$  of the virtual gluon and quark in the corresponding Feynman diagrams. But because we want to estimate  $\sim 1/Q^{2n}$ ,  $n = 1, 2, \dots$  corrections to the form factor, we shall use Eq. (2.32) for the calculation of  $Q^2F_{\eta'g^*g^*}(Q^2, \omega)$  as well.

The next problem then is how to generalize Eqs. (2.21) and (2.22) in such a way so that the corresponding hard-scattering amplitudes  $T_{1(2)}^{q(g)}$  and the quark and gluon components of the vertex function will obey Eqs. (2.25-2.31). For this purpose, we symmetrize the functions  $T_{1(2)}^{q(g)}(x, Q^2, \omega, \mu_R^2, \overline{\mu}_R^2)$  by exchanging  $\mu_R^2 \leftrightarrow \overline{\mu}_R^2$

$$\begin{aligned} T_1^q(x, Q^2, \omega) &= \frac{1}{2} \left[ T_1^q(x, Q^2, \omega, \mu_R^2) + T_1^q(x, Q^2, \omega, \overline{\mu}_R^2) \right] \\ &= -\frac{2\pi}{3Q^2} \frac{\alpha_s(Q^2x) + \alpha_s(Q^2\overline{x})}{(1+\omega)x + (1-\omega)\overline{x}}, \\ T_2^q(x, Q^2, \omega) &= \frac{1}{2} \left[ T_2^q(x, Q^2, \omega, \overline{\mu}_R^2) + T_2^q(x, Q^2, \omega, \mu_R^2) \right] \\ &= -\frac{2\pi}{3Q^2} \frac{\alpha_s(Q^2x) + \alpha_s(Q^2\overline{x})}{(1+\omega)\overline{x} + (1-\omega)x} \end{aligned} \quad (2.33)$$

and

$$\begin{aligned}
T_1^g(x, Q^2, \omega) &= \frac{1}{2} \left[ T_1^g(x, Q^2, \omega, \mu_R^2) + T_1^g(x, Q^2, \omega, \bar{\mu}_R^2) \right] \\
&= \frac{\pi}{2Q^2 n_f} \left[ \alpha_s(Q^2 x) + \alpha_s(Q^2 \bar{x}) \right] \frac{(1+\omega)x + (1-\omega)\bar{x}}{\omega [(1+\omega)\bar{x} + (1-\omega)x]}, \\
T_2^g(x, Q^2, \omega) &= \frac{1}{2} \left[ T_2^g(x, Q^2, \omega, \bar{\mu}_R^2) + T_2^g(x, Q^2, \omega, \mu_R^2) \right] \\
&= \frac{\pi}{2Q^2 n_f} \left[ \alpha_s(Q^2 x) + \alpha_s(Q^2 \bar{x}) \right] \frac{(1+\omega)\bar{x} + (1-\omega)x}{\omega [(1+\omega)x + (1-\omega)\bar{x}]}.
\end{aligned} \tag{2.34}$$

In the “frozen” coupling-constant approximation  $Q^2 x, Q^2 \bar{x} \rightarrow Q^2$ , Eqs. (2.33) and (2.34) coincide with expressions (2.21) and (2.22). It is also not difficult to verify that the hard-scattering amplitudes  $T_{1(2)}^{q(g)}(x, Q^2, \omega)$  (2.33), (2.34) satisfy Eqs. (2.25) and (2.26). As a result, Eqs. (2.27)-(2.31) remain valid also within the RC method.

### C. Quark and gluon components of the $\eta'$ meson distribution amplitude

The important input information needed for the computation of the form factor  $F_{\eta' g^* g^*}(Q^2, \omega)$  are the DA’s of the quark and gluon components of the  $\eta'$  meson, namely, the functions  $\phi^q(x, Q^2)$  and  $\phi^g(x, Q^2)$ . In general, a meson DA is a function containing all nonperturbative, long-distance effects, which cannot be calculated by employing perturbative QCD tools. Its dependence on  $x$  (or its shape) has to be deduced from experimental data or found using some nonperturbative methods, for example, QCD sum-rules (see, e.g., [46]). In contrast, the evolution of the DA with the factorization scale  $Q^2$  is governed by PQCD.

The evolution equation for a flavor singlet pseudoscalar meson was derived and solved in Refs. [9, 10, 11]. It turned out that due to mixing of the quark-antiquark and two-gluon components of the meson DA, the evolution equation has a  $(2 \times 2)$  matrix form. The anomalous dimensions matrix, which enters into the evolution equation at the one-loop order, has the following components [9, 10, 11] (see also Ref. [47])

$$\begin{aligned}
\gamma_{qq}^n &= C_F \left[ 3 + \frac{2}{(n+1)(n+2)} - 4 \sum_{j=1}^{n+1} \frac{1}{j} \right], \quad \gamma_{gg}^n = N_c \left[ \frac{\beta_0}{N_c} + \frac{8}{(n+1)(n+2)} - 4 \sum_{j=1}^{n+1} \frac{1}{j} \right], \\
\gamma_{qg}^n &= \frac{12n_f}{(n+1)(n+2)}, \quad \gamma_{gq}^n = C_F \frac{n(n+3)}{3(n+1)(n+2)},
\end{aligned} \tag{2.35}$$

where  $N_c = 3$  and  $C_F = 4/3$  is the group theoretical factor for  $SU_c(3)$ . The anomalous dimensions matrix has the eigenvalues

$$\gamma_{\pm}^n = \frac{1}{2} \left[ \gamma_{qq}^n + \gamma_{gg}^n \pm \sqrt{(\gamma_{qq}^n - \gamma_{gg}^n)^2 + 4\gamma_{qg}^n \gamma_{gq}^n} \right]. \tag{2.36}$$

The solutions of the evolution equation for the (singlet) quark and gluon components of the DA has, in general, the form

$$\phi^q(x, Q^2) = 6Cx\bar{x} \left\{ 1 + \sum_{k=2,4..}^{\infty} \left[ B_n^q \left( \frac{\alpha_s(\mu_0^2)}{\alpha_s(Q^2)} \right)^{\frac{\gamma_+^n}{\beta_0}} + \rho_n^g B_n^g \left( \frac{\alpha_s(\mu_0^2)}{\alpha_s(Q^2)} \right)^{\frac{\gamma_-^n}{\beta_0}} \right] C_n^{3/2}(x - \bar{x}) \right\}, \quad (2.37)$$

and

$$\phi^g(x, Q^2) = Cx\bar{x} \sum_{k=2,4..}^{\infty} \left[ \rho_n^g B_n^g \left( \frac{\alpha_s(\mu_0^2)}{\alpha_s(Q^2)} \right)^{\frac{\gamma_+^n}{\beta_0}} + B_n^g \left( \frac{\alpha_s(\mu_0^2)}{\alpha_s(Q^2)} \right)^{\frac{\gamma_-^n}{\beta_0}} \right] C_{n-1}^{5/2}(x - \bar{x}), \quad (2.38)$$

with the constant  $C$  being defined as

$$C = \sqrt{2}f_q \sin \phi_p + f_s \cos \phi_p.$$

In Eqs. (2.37) and (2.38)  $C_n^{3/2}(z)$  and  $C_n^{5/2}(z)$  are Gegenbauer polynomials, calculable using the recurrence formula [48]

$$(n+1)C_{n+1}^{\nu}(z) = 2(n+\nu)zC_n^{\nu}(z) - (n+2\nu-1)C_{n-1}^{\nu}(z), \quad (2.39)$$

$$C_0^{\nu}(z) = 1, \quad C_1^{\nu}(z) = 2\nu z.$$

The parameters  $\rho_n^q$  and  $\rho_n^g$  are determined in terms of the anomalous dimensions matrix elements

$$\rho_n^q = 6 \frac{\gamma_+^n - \gamma_{qq}^n}{\gamma_{gg}^n}, \quad \rho_n^g = \frac{1}{6} \frac{\gamma_{gg}^n}{\gamma_-^n - \gamma_{qq}^n}. \quad (2.40)$$

In Eqs. (2.37) and (2.38)  $\mu_0 = 0.5$  GeV is the normalization point, at which the free input parameters  $B_n^q$ ,  $B_n^g$  in the DA's  $\phi^q(x, Q^2)$  and  $\phi^g(x, Q^2)$  have to be fixed. Exactly these parameters determine the shape of the DA's.

For all  $n \geq 2$ , the eigenvalues  $\gamma_{\pm}^n < 0$  and their absolute values increase with  $n$ . Hence, in the asymptotic limit  $Q^2 \rightarrow \infty$ , one has

$$\left( \frac{\alpha_s(\mu_0^2)}{\alpha_s(Q^2)} \right)^{\frac{\gamma_+^n(\gamma_-^n)}{\beta_0}} \sim \ln \left( Q^2 / \Lambda^2 \right)^{\frac{\gamma_+^n(\gamma_-^n)}{\beta_0}} \rightarrow 0$$

and therefore only the quark component of the  $\eta'$  meson DA survives, evolving to its asymptotic form, whereas the gluon DA in this limit vanishes,

$$\phi^q(x, Q^2) \xrightarrow{Q^2 \rightarrow \infty} 6Cx\bar{x}, \quad \phi^g(x, Q^2) \xrightarrow{Q^2 \rightarrow \infty} 0. \quad (2.41)$$

In this work, we shall use the  $\eta'$ -meson DA that contains only the first non-asymptotic terms. In other words, we suggest that in Eqs. (2.37) and (2.38)  $B_2^q \neq 0$ ,  $B_2^g \neq 0$  and  $B_n^q = B_n^g = 0$  for all  $n \geq 4$ . The numerical values of the relevant parameters for  $n_f = 3$  are

$$\gamma_{qq}^2 = -\frac{50}{9}, \quad \gamma_{gg}^2 = -11, \quad \gamma_{qg}^2 = \frac{10}{27}, \quad \gamma_{gq}^2 = 3,$$

$$\gamma_+^2 \simeq -\frac{48}{9}, \quad \gamma_-^2 \simeq -\frac{101}{9}, \quad \rho_2^q \simeq \frac{16}{5}, \quad \rho_2^g \simeq -\frac{1}{90}. \quad (2.42)$$

Taking into account Eq. (2.42) and the expressions for the required Gegenbauer polynomials

$$C_2^{3/2}(x - \bar{x}) = \frac{3}{2} [5(x - \bar{x})^2 - 1] = 6(1 - 5x\bar{x}), \quad C_1^{5/2}(x - \bar{x}) = 5(x - \bar{x}),$$

we finally recast the  $\eta'$  meson quark and gluon DA's into the more suitable (for our purposes) forms

$$\phi^q(x, Q^2) = 6Cx\bar{x} [1 + A(Q^2) - 5A(Q^2)x\bar{x}], \quad \phi^g(x, Q^2) = Cx\bar{x}(x - \bar{x})B(Q^2). \quad (2.43)$$

In the above, the functions  $A(Q^2)$  and  $B(Q^2)$  are defined by

$$\begin{aligned} A(Q^2) &= 6B_2^q \left( \frac{\alpha_s(Q^2)}{\alpha_s(\mu_0^2)} \right)^{\frac{48}{81}} - \frac{B_2^g}{15} \left( \frac{\alpha_s(Q^2)}{\alpha_s(\mu_0^2)} \right)^{\frac{101}{81}}, \\ B(Q^2) &= 16B_2^q \left( \frac{\alpha_s(Q^2)}{\alpha_s(\mu_0^2)} \right)^{\frac{48}{81}} + 5B_2^g \left( \frac{\alpha_s(Q^2)}{\alpha_s(\mu_0^2)} \right)^{\frac{101}{81}}. \end{aligned} \quad (2.44)$$

Equations (2.43) and (2.44) together with Eq. (2.9) contain all necessary information about the  $\eta'$  meson DA.

### III. RUNNING COUPLING METHOD AND POWER SUPPRESSED CORRECTIONS

To compute the  $\eta'$  meson -virtual gluon transition form factor  $F_{\eta' g^* g^*}(Q^2, \omega)$ , we have to perform in Eqs. (2.16) and (2.17) the integration over  $x$  by inserting the explicit expressions for the hard-scattering amplitudes  $T_{1,2}^{q(g)}(x, Q^2, \omega)$ , the  $\eta'$ -meson quark and gluon DA's and retain the  $x$ -dependence of the coupling  $\alpha_s(Q^2 x)$  [ $\alpha_s(Q^2 \bar{x})$ ]. Such calculations lead to divergent integrals because the running coupling  $\alpha_s(Q^2 x)$  [ $\alpha_s(Q^2 \bar{x})$ ] suffers from an infrared singularity in the limit  $x \rightarrow 0$  [ $x \rightarrow 1$ ]. This means that in order to carry out computations with the running coupling, some procedure for its regularization in the end-point  $x \rightarrow 0, 1$  regions has to be adopted.

As a first step in this direction, we express the running coupling  $\alpha_s(Q^2 \lambda)$  in terms of  $\alpha_s(Q^2)$ , employing the renormalization-group equation

$$\frac{\partial \alpha_s(Q^2 \lambda)}{\partial \ln \lambda} = -\frac{\beta_0}{4\pi} [\alpha_s(Q^2 \lambda)]^2 - \frac{\beta_1}{8\pi^2} [\alpha_s(Q^2 \lambda)]^3. \quad (3.1)$$

The solution of Eq. (3.1), obtained by keeping the leading  $(\alpha_s \ln \lambda)^k$  and next-to-leading  $\alpha_s(\alpha_s \ln \lambda)^{k-1}$  powers of  $\ln \lambda$ , reads [49]

$$\alpha_s(Q^2 \lambda) \simeq \frac{\alpha_s(Q^2)}{1 + \ln \lambda/t} \left[ 1 - \frac{\alpha_s(Q^2) \beta_1}{2\pi \beta_0} \frac{\ln[1 + \ln \lambda/t]}{1 + \ln \lambda/t} \right], \quad (3.2)$$

where  $\alpha_s(Q^2)$  is the one-loop QCD coupling constant and  $t = 4\pi/\beta_0 \alpha_s(Q^2)$ .

Inserting Eq. (3.2) into the expressions for the hard-scattering amplitudes and subsequently  $T_{1,2}^{q(g)}(x, Q^2, \omega)$  into Eqs. (2.16) and (2.17), we obtain integrals which are still divergent, but which now can be calculated using existing methods. One of these methods, applied in Ref. [28] for the calculation of the electromagnetic pion form factor, allows us to find the quantity under consideration as a perturbative series in  $\alpha_s(Q^2)$  with factorially growing coefficients  $C_n \sim (n-1)!$ . Similar series with coefficients  $C_n \sim (n-1)!$  may be found also for the form factor  $Q^2 F_{\eta' g^* g^*}(Q^2, \omega)$ , i.e.,

$$Q^2 F_{\eta' g^* g^*}(Q^2, \omega) \sim \sum_{n=1}^{\infty} \left[ \frac{\alpha_s(Q^2)}{4\pi} \right]^n \beta_0^{n-1} C_n. \quad (3.3)$$

But a perturbative QCD series with factorially growing coefficients is a signal for the IR renormalon nature of the divergences in Eq. (3.3). The convergence radius of the series (3.3) is zero and its resummation should be performed by employing the Borel integral technique. First, one has to find the Borel transform  $B[Q^2 F_{\eta' g^* g^*}](u)$  of the corresponding series [50]

$$B[Q^2 F_{\eta' g^* g^*}](u) = \sum_{n=1}^{\infty} \frac{u^{n-1}}{(n-1)!} C_n. \quad (3.4)$$

Because the coefficients of the series (3.3) behave like  $C_n \sim (n-1)!$ , the Borel transform (3.4) contains poles located at the positive  $u$  axis of the Borel plane. In other words, the divergence of the series (3.3) owing to Eq. (3.4) has been transformed into pole-like singularities of the function  $B[Q^2 F_{\eta' g^* g^*}](u)$ . These poles are the footprints of the IR renormalons.

Now in order to define the sum (3.3) or to find the resummed expression for the form factor, one has to invert  $B[Q^2 F_{\eta' g^* g^*}](u)$  to get

$$[Q^2 F_{\eta' g^* g^*}(Q^2, \omega)]^{res} \sim P.V. \int_0^{\infty} du \exp \left[ -\frac{4\pi}{\beta_0 \alpha_s(Q^2)} u \right] B[Q^2 F_{\eta' g^* g^*}](u), \quad (3.5)$$

and remove the IR renormalon divergences by the principal value prescription.

The procedure described above, is straightforward but, at the same time, tedious. Fortunately, these intermediate operations can be bypassed by introducing the inverse Laplace transforms of the functions in Eq. (3.2) [51], viz.,

$$\frac{1}{(t+z)^{\nu}} = \frac{1}{\Gamma(\nu)} \int_0^{\infty} du \exp[-u(t+z)] u^{\nu-1}, \quad Re\nu > 0, \quad (3.6)$$

and

$$\frac{\ln(t+z)}{(t+z)^2} = \int_0^{\infty} du \exp[-u(t+z)] (1 - \gamma_E - \ln u) u, \quad (3.7)$$

where  $\Gamma(z)$  is the Gamma function,  $\gamma_E \simeq 0.577216$  is the Euler constant and  $z = \ln x$  [or  $z = \ln \bar{x}$ ].

Then using Eqs. (3.2), (3.6) and (3.7) for  $\alpha_s(Q^2 \lambda)$ , we get [6]

$$\alpha_s(Q^2 \lambda) = \alpha_s(Q^2) t \int_0^{\infty} du \exp(-ut) \lambda^{-u} R(u, t) = \frac{4\pi}{\beta_0} \int_0^{\infty} du \exp(-ut) \lambda^{-u} R(u, t), \quad (3.8)$$

with the function  $R(u, t)$  defined as

$$R(u, t) = 1 - \frac{2\beta_1}{\beta_0^2} u(1 - \gamma_E - \ln t - \ln u). \quad (3.9)$$

Employing Eq. (3.8) for  $\alpha_s(Q^2\lambda)$  and carrying out the integrations over  $x$ , we obtain (see, the next Section) the quark and gluon components of the form factor  $F_{\eta'g^*g^*}(Q^2, \omega)$  directly in the Borel resummed form (3.5).

The resummed vertex function  $[Q^2 F_{\eta'g^*g^*}(Q^2, \omega)]^{res}$  - except for the  $\eta'$  meson - on-shell gluon transition and the  $\omega = 0$  case - contains an infinite number of IR renormalon poles located at  $u_0 = n$ , where  $n$  is a positive integer that, in general, is given as a sum of a series, i.e.,

$$S(k_0, Q^2, \omega) \sim \sum_{n=k_0}^{\infty} \frac{4\pi}{\beta_0} P.V. \int_0^{\infty} \frac{e^{-ut} R(u, t) du}{n-u} C_n(\omega). \quad (3.10)$$

One appreciates that all information on the process asymmetry parameter  $\omega$  is accumulated in the coefficient functions  $C_n(\omega)$ .

To avoid inessential technical details and to make the presentation as transparent as possible, let us for the time being neglect the non-leading term  $\sim \alpha_s^2$  in Eq. (3.2) and make the replacement  $R(u, t) \rightarrow 1$  in Eq. (3.10). Then, the integrals in Eq. (3.10) take, after simple manipulations, the form

$$\frac{4\pi}{\beta_0} P.V. \int_0^{\infty} \frac{e^{-ut} du}{n-u} = \frac{4\pi}{\beta_0} \frac{li(\lambda^n)}{\lambda^n}, \quad \lambda = Q^2/\Lambda^2, \quad (3.11)$$

with the logarithmic integral  $li(x)$  defined by

$$li(x) = P.V. \int_0^x \frac{dt}{\ln t}. \quad (3.12)$$

The function  $li(x)$  is expressible in terms of the function  $E_1(z)$  [48]

$$li(x) = -E_1(-\ln x), \quad (3.13)$$

where

$$E_1(z) = \int_z^{\infty} e^{-t} t^{-1} dt.$$

The latter expression can, for  $|z| \rightarrow \infty$ , be expanded over inverse powers of  $z$

$$E_1(z) = z^{-1} e^{-z} \left[ \sum_{m=0}^M \frac{m!}{(-z)^m} + O(|z|^{-(M+1)}) \right]. \quad (3.14)$$

Using Eqs. (3.13) and (3.14), we find

$$li(x) \simeq \frac{x}{\ln x} \sum_{m=0}^M \frac{m!}{(\ln x)^m}, \quad \frac{li(x^n)}{x^n} \simeq \frac{1}{n \ln x} \sum_{m=0}^M \frac{m!}{(n \ln x)^m}. \quad (3.15)$$

It is not difficult to see that for  $Q^2 \gg \Lambda^2$

$$\frac{4\pi}{\beta_0} \frac{li(\lambda^n)}{\lambda^n} \simeq 4\pi \sum_{m=1}^M \left[ \frac{\alpha_s(Q^2)}{4\pi} \right]^m \beta_0^{m-1} \frac{(m-1)!}{n^m}. \quad (3.16)$$

Choosing in Eq. (3.16)  $M \rightarrow \infty$  and comparing the obtained result with Eq. (3.3), we conclude that each term in the sum (3.10) at fixed  $n$  is the resummed Borel expression of the series (3.16).

But we can look at the integrals in Eq. (3.10) from another side. Namely, it is easy to show that

$$\frac{4\pi}{\beta_0} \int_0^\infty \frac{e^{-ut} du}{n-u} = \int_0^1 \alpha_s(Q^2 x) x^{n-1} dx = \frac{1}{n} f_{2n}(Q), \quad (3.17)$$

where  $f_{2n}(Q)$  are the moment integrals

$$f_p(Q) = \frac{p}{Q^p} \int_0^Q dk k^{p-1} \alpha_s(k^2). \quad (3.18)$$

The integrals  $f_p(Q)$  can be calculated using the IR matching scheme [52]

$$f_p(Q) = \left( \frac{\mu_I}{Q} \right)^p f_p(\mu_I) + \alpha_s(Q^2) \sum_{n=0}^N \left[ \frac{\beta_0}{2\pi p} \alpha_s(Q^2) \right]^n [n! - \Gamma(n+1, p \ln(Q/\mu_I))]. \quad (3.19)$$

where  $\mu_I$  is the infrared matching scale and  $\Gamma(n+1, z)$  is the incomplete Gamma function

$$\Gamma(n+1, z) = \int_z^\infty e^{-t} t^n dt. \quad (3.20)$$

In Eq. (3.19)  $f_p(\mu_I)$  are phenomenological parameters, which represent the weighted average of  $\alpha_s(k^2)$  over the IR region  $0 < k < \mu_I$  and act at the same time as infrared regulators of the r.h.s. of Eq. (3.17). The first term on the r.h.s. of Eq. (3.19) is a power-suppressed contribution to  $f_p(Q)$ , which cannot be calculated within PQCD, whereas the second term is the perturbatively calculable part of the function  $f_p(Q)$ . Stated differently, the infrared matching scheme allows one to estimate power corrections to the moment integrals by explicitly dissecting them from the full expression and introducing new nonperturbative parameters  $f_p(\mu_I)$ . The values of these parameters have to be extracted from experimental data.

In order to check the accuracy of both the RC method (IR renormalon calculus) and the infrared matching scheme, in Ref. [52], the Landau-pole free model for  $\alpha_s(Q^2)$  was introduced, yielding

$$\alpha_s(Q^2) = \frac{4\pi}{\beta_0} \left[ \frac{1}{\ln \lambda} + 125 \frac{1+4\lambda}{(1-\lambda)(4+\lambda)^4} \right]. \quad (3.21)$$

The model expression (3.21) was used for the exact calculation of the moment integrals  $f_p^{\text{exact}}(Q)$ . The IR renormalon and the IR matching scheme results were compared with  $f_p^{\text{exact}}(Q)$  concluding that for  $N \geq 2$  the IR matching scheme leads to a good agreement with the exact values of  $f_p(Q)$ . As regards the calculation of the integrals  $f_p(Q)$ , when employing the RC method with the principal value prescription, a good agreement with  $f_2^{\text{exact}}(Q)$  was found for  $p = 2$ , while for  $p = 1$  a small deviation from  $f_1^{\text{exact}}(Q)$  in the region of  $Q^2 \sim \text{a few GeV}^2$  was observed (the lowest moment integral entering into our expressions is  $f_2(Q)$ ). But even for  $p = 1$ , the agreement with  $f_1^{\text{exact}}(Q)$  within the error bars is quite satisfactory in view of the uncertainties produced by the principal value prescription itself. Therefore, we can conclude that the RC method and the IR matching scheme lead for the moment integrals  $f_p(Q)$  to approximately similar numerical results. It is remarkable that in

both cases an enhancement of the IR renormalon and matching-scheme results relative to the leading-order perturbative prediction was found.

After presenting our analysis, it becomes evident that the Borel resummation technique enables us to estimate with a rather good accuracy power-behaved corrections to the integrals in Eq. (3.10) and hence to the vertex function  $F_{\eta'g^*g^*}(Q^2, \omega)$ . Of course, one can employ the IR matching scheme and Eq. (3.19) to determine power corrections to the form factor in explicit form. But as we have noted above, in general, the form factor  $Q^2 F_{\eta'g^*g^*}(Q^2, \omega)$  contains an infinite number of IR renormalon poles or stated equivalently, an infinite number of  $f_{2n}(Q)$  is required to calculate sums like the one presented in Eq. (3.10). In real numerical computations, in order to reach a good approximation of the series (3.10), at least a sum of the first  $15 \div 20$  terms is needed, meaning the involvement of  $f_{2n}(\mu_I)$  ( $n = 15 \div 20$ ) nonperturbative parameters. But from the experimental data, only the first few moments  $f_p(\mu_I)$  could be extracted [53, 54, 55, 56]. Values for  $f_1(2 \text{ GeV})$  (in the literature the notation  $f_1(\mu_I) = \alpha_0(\mu_I)$  is widely used) range from  $\alpha_0(2 \text{ GeV}) = 0.435 \pm 0.021$  [53] and  $\alpha_0(2 \text{ GeV}) = 0.513^{+0.066}_{-0.045}$  [54] to  $\alpha_0(2 \text{ GeV}) = 0.597^{+0.009}_{-0.010}$  [55]. Here, we write down only sample results, obtained in these works, in order to demonstrate the experimental situation with  $\alpha_0(2 \text{ GeV}) = f_1(2 \text{ GeV})$ . For  $f_2(2 \text{ GeV})$  the value  $f_2(2 \text{ GeV}) \simeq 0.5$  was deduced [52, 57] from the data on structure functions [56].

In the framework of the RC method, we estimate the same power corrections to a physical quantity, but here we do not need additional information on  $f_p(\mu_I)$ . Moreover, this method gives us the possibility to calculate values of the nonperturbative parameters  $f_p(\mu_I)$  by means of the formula

$$f_{2n}(\mu_I) = n \frac{4\pi}{\beta_0} \frac{\text{li}(\tilde{\lambda}^n)}{\tilde{\lambda}^n}, \quad \tilde{\lambda} = \mu_I^2/\Lambda^2, \quad (3.22)$$

that can be easily found by comparing Eqs. (3.11) and (3.17). The calculated values of the first few even moments ( $n_f = 3$ ,  $\Lambda = 0.3 \text{ GeV}$ ) are

$$f_2(2 \text{ GeV}) \simeq 0.535, \quad f_4(2 \text{ GeV}) \simeq 0.45, \quad f_6(2 \text{ GeV}) \simeq 0.41. \quad (3.23)$$

To compare our predictions with those computed via the model  $\alpha_s(Q^2)$  (Eq. (3.21)), we choose  $n_f = 3$  and  $\Lambda = 0.25 \text{ GeV}$ . The corresponding values are shown below

$$\begin{aligned} f_2^{\text{RC}}(2 \text{ GeV}) &\simeq 0.479, & f_4^{\text{RC}}(2 \text{ GeV}) &\simeq 0.393, \\ f_2^{\text{mod}}(2 \text{ GeV}) &\simeq 0.450, & f_4^{\text{mod}}(2 \text{ GeV}) &\simeq 0.388. \end{aligned} \quad (3.24)$$

One observes that the parameters  $f_p(\mu_I)$  of the RC method are in agreement with both the experimental results and the model calculations.

We have noted above that the principal value prescription, adopted in this work in order to regularize divergent integrals (see, Eqs. (3.5), (3.10)) generates power-suppressed uncertainties  $\sim \frac{1}{Q^{2q}} \Phi_q(Q^2)$ , where  $\{\Phi_q(Q^2)\}$  are calculable functions entirely fixed by the residues of the Borel transform  $B[Q^2 F_{Mg^*g^*}](u)$  at the poles  $q = u_0$ . These uncertainties have to be cancelled by ultraviolet (UV) renormalon ambiguities arising from higher-twist contributions to  $Q^2 F_{Mg^*g^*}(Q^2, \omega)$ . In accordance with the UV dominance assumption [26], not only the uncertainties but the whole higher-twist corrections to  $Q^2 F_{Mg^*g^*}(Q^2, \omega)$  must be proportional to

$$\sim \sum_q N_q \frac{\Phi_q(Q^2)}{Q^{2q}}, \quad (3.25)$$

where  $\{N_q\}$  are arbitrary constants to be fixed from experimental data. In Ref. [6] the corrections (3.25) to the  $\eta'\gamma$  electromagnetic transition form factor  $Q^2 F_{\eta'\gamma}(Q^2)$  were estimated. For the  $\eta'$  meson asymptotic DA and for the parameters  $N_1 = N_2 = 1$  and  $N_1 = N_2 = -1$ , it was found that they do not exceed  $\pm 15\%$  of the  $\eta'\gamma$  form factor. Because the RC method allows us to evaluate power corrections to a physical quantity and for the  $\eta'\gamma$  transition form factor led to a good agreement with the CLEO data [1], one should introduce the constraint  $|N_{1,2}| \ll 1$  in order to retain this agreement. Assuming that similar estimations for  $N_q$  are valid also in the case of the  $\eta'g$  and  $\eta'g^*$  transitions, we neglect in this work uncertainties produced by the principal value prescription.

#### IV. THE FORM FACTOR $F_{\eta'g^*g^*}(Q^2, \omega)$ WITHIN THE RC METHOD

In this section we calculate the quark and gluon components of the vertex function  $F_{\eta'g^*g^*}(Q^2, \omega)$  within the RC method. We also present our results for  $F_{\eta'gg^*}(Q^2, \omega = \pm 1)$ ,  $F_{\eta'g^*g^*}(Q^2, \omega = 0)$  and the asymptotic limit for the form factor.

##### A. Quark component $F_{\eta'g^*g^*}^q(Q^2, \omega)$ of the vertex function

To calculate the quark component of the vertex function  $F_{\eta'g^*g^*}^q(Q^2, \omega)$ , we use Eq. (2.28) for  $F_{\eta'g^*g^*}^q(Q^2, \omega)$ , Eq. (2.33) for the hard scattering amplitude  $T_1^q(x, Q^2, \omega)$ , and the expression for  $\alpha_s(\lambda Q^2)$  given in Eq. (3.8). Employing the quark component of the  $\eta'$ -meson DA,  $\phi^q(x, Q^2)$ , we get<sup>3</sup>

$$\begin{aligned} Q^2 F_{\eta'g^*g^*}^q(Q^2, \omega) = & -\frac{32\pi^2 C[1 + A(Q^2)]}{\beta_0} \int_0^\infty du e^{-ut} R(u, t) \\ & \times \left[ \int_0^1 \frac{x^{1-u} \bar{x} dx}{(1+\omega)x + (1-\omega)\bar{x}} + \int_0^1 \frac{x\bar{x}^{1-u} dx}{(1+\omega)x + (1-\omega)\bar{x}} \right] \\ & + \frac{160\pi^2 C A(Q^2)}{\beta_0} \int_0^\infty du e^{-ut} R(u, t) \left[ \int_0^1 \frac{x^{2-u} \bar{x}^2 dx}{(1+\omega)x + (1-\omega)\bar{x}} \right. \\ & \left. + \int_0^1 \frac{x^2 \bar{x}^{2-u} dx}{(1+\omega)x + (1-\omega)\bar{x}} \right]. \end{aligned} \quad (4.1)$$

Using the fact that the integral [58]

$$\int_0^1 x^{\alpha-1} \bar{x}^{\beta-1} (1-xr)^\gamma dx = B(\alpha, \beta) {}_2F_1(-\gamma, \alpha; \alpha + \beta; r) \quad (4.2)$$

is expressible in terms of the Gauss hypergeometric function [59]

$${}_2F_1(a, b; c; z) = \sum_{k=0}^{\infty} \frac{(a)_k (b)_k}{(c)_k} \frac{z^k}{k!}, \quad (4.3)$$

---

<sup>3</sup> In what follows integrals over the variable  $u$  have to be understood in the sense of the Cauchy principal value.

we obtain

$$\begin{aligned}
Q^2 F_{\eta' g^* g^*}^q(Q^2, \omega) = & -\frac{32\pi^2 C[1 + A(Q^2)]}{\beta_0(1 - \omega)} \int_0^\infty du e^{-ut} R(u, t) B(2 - u, 2) \\
& \times \left[ {}_2F_1 \left( 1, 2 - u; 4 - u; -\frac{2\omega}{1 - \omega} \right) + {}_2F_1 \left( 1, 2; 4 - u; -\frac{2\omega}{1 - \omega} \right) \right] \\
& + \frac{160\pi^2 C A(Q^2)}{\beta_0(1 - \omega)} \int_0^\infty du e^{-ut} R(u, t) B(3 - u, 3) \left[ {}_2F_1 \left( 1, 3 - u; 6 - u; -\frac{2\omega}{1 - \omega} \right) \right. \\
& \left. + {}_2F_1 \left( 1, 3; 6 - u; -\frac{2\omega}{1 - \omega} \right) \right]. \tag{4.4}
\end{aligned}$$

In Eqs. (4.2) and (4.3),  $B(x, y)$  and  $(a)_n$  are the Beta function and Pochhammer symbols, respectively, defined in terms of the Gamma function  $\Gamma(z)$

$$B(x, y) = \frac{\Gamma(x)\Gamma(y)}{\Gamma(x+y)}, \quad (a)_n = \frac{\Gamma(a+n)}{\Gamma(a)}.$$

Applying the transformation property of the Gauss function  ${}_2F_1(a, b; c; z)$  [59],

$${}_2F_1(a, b; c; z) = (1 - z)^{-a} {}_2F_1 \left( a, c - b; c; \frac{z}{z - 1} \right), \tag{4.5}$$

we can obtain the alternative expression for the form factor  $F_{\eta' g^* g^*}^q(Q^2, \omega)$ , viz.,

$$\begin{aligned}
Q^2 F_{\eta' g^* g^*}^q(Q^2, \omega) = & -\frac{32\pi^2 C[1 + A(Q^2)]}{\beta_0(1 + \omega)} \int_0^\infty du e^{-ut} R(u, t) B(2 - u, 2) \\
& \times \left[ {}_2F_1 \left( 1, 2; 4 - u; \frac{2\omega}{1 + \omega} \right) + {}_2F_1 \left( 1, 2 - u; 4 - u; \frac{2\omega}{1 + \omega} \right) \right] \\
& + \frac{160\pi^2 C A(Q^2)}{\beta_0(1 + \omega)} \int_0^\infty du e^{-ut} R(u, t) B(3 - u, 3) \left[ {}_2F_1 \left( 1, 3; 6 - u; \frac{2\omega}{1 + \omega} \right) \right. \\
& \left. + {}_2F_1 \left( 1, 3 - u; 6 - u; \frac{2\omega}{1 + \omega} \right) \right]. \tag{4.6}
\end{aligned}$$

From Eqs. (4.4) and (4.6) a simple expression for the  $\eta'$  meson-on-shell gluon transition form factor  $F_{\eta' gg^*}^q(Q^2, \omega = \pm 1)$  can be found

$$\begin{aligned}
Q^2 F_{\eta' gg^*}^q(Q^2, \omega = \pm 1) = & -\frac{16\pi^2 C[1 + A(Q^2)]}{\beta_0} \int_0^\infty du e^{-ut} R(u, t) [B(1, 2 - u) \\
& + B(2, 1 - u)] + \frac{80\pi^2 C A(Q^2)}{\beta_0} \int_0^\infty du e^{-ut} R(u, t) [B(3, 2 - u) + B(2, 3 - u)], \tag{4.7}
\end{aligned}$$

where we have used the equality [59]

$${}_2F_1(a, b; c; 1) = \frac{\Gamma(c)\Gamma(c - a - b)}{\Gamma(c - a)\Gamma(c - b)}. \tag{4.8}$$

It is worth noting that Eq. (4.7) can be obtained from the first equality in Eq. (2.27) by employing the  $\omega \rightarrow \pm 1$  limits of the hard scattering amplitudes (2.33)

$$T_1^q(x, Q^2, \omega = \pm 1) + T_2^q(x, Q^2, \omega = \pm 1) = -\frac{\pi}{3Q^2} [\alpha_s(Q^2 x) + \alpha_s(Q^2 \bar{x})] \left[ \frac{1}{x} + \frac{1}{\bar{x}} \right]. \quad (4.9)$$

In the case of gluons with equal virtualities  $Q_1^2 = Q_2^2$  and hence, in the  $\omega = 0$  case, the form factor can be found employing the expression for the hard-scattering amplitude

$$T_1^q(x, Q^2, \omega = 0) + T_2^q(x, Q^2, \omega = 0) = -\frac{4\pi}{3Q^2} [\alpha_s(Q^2 x) + \alpha_s(Q^2 \bar{x})]. \quad (4.10)$$

Calculation leads to the simple expression

$$\begin{aligned} Q^2 F_{\eta' g^* g^*}^q(Q^2, \omega = 0) &= -\frac{64\pi^2 C(1 + A(Q^2))}{\beta_0} \int_0^\infty du e^{-ut} R(u, t) B(2 - u, 2) \\ &\quad + \frac{320\pi^2 C A(Q^2)}{\beta_0} \int_0^\infty du e^{-ut} R(u, t) B(3 - u, 3). \end{aligned} \quad (4.11)$$

Let us note that Eq. (4.11) can be deduced from both Eqs. (4.4) and (4.6) in the limit  $\omega \rightarrow 0$  by taking into account that [59]

$${}_2F_1(a, b; c; 0) = 1.$$

The next important problem to be solved within the framework of the RC method, is to reveal the IR renormalon poles in Eqs. (4.4), (4.6), (4.7) and (4.11) because without such a clarification all these expressions would have merely a formal character.

We start from the simple case, i.e., from Eq. (4.7) and get

$$\begin{aligned} B(1, 2 - u) + B(2, 1 - u) &= \frac{\Gamma(1)\Gamma(2 - u)}{\Gamma(3 - u)} + \frac{\Gamma(2)\Gamma(1 - u)}{\Gamma(3 - u)} \\ &= \frac{1}{2 - u} + \frac{1}{(1 - u)(2 - u)} = \frac{1}{1 - u} \end{aligned}$$

and

$$\begin{aligned} B(3, 2 - u) + B(2, 3 - u) &= \frac{\Gamma(3)\Gamma(2 - u)}{\Gamma(5 - u)} + \frac{\Gamma(2)\Gamma(3 - u)}{\Gamma(5 - u)} \\ &= \frac{2}{(2 - u)(3 - u)(4 - u)} + \frac{1}{(3 - u)(4 - u)} = \frac{1}{2 - u} - \frac{1}{3 - u}. \end{aligned}$$

In deriving these expressions we used the following property of the Gamma function

$$z\Gamma(z) = \Gamma(z + 1).$$

Hence we have

$$\begin{aligned} Q^2 F_{\eta' gg^*}^q(Q^2, \omega = \pm 1) &= -\frac{16\pi^2 C[1 + A(Q^2)]}{\beta_0} \int_0^\infty e^{-ut} R(u, t) \frac{du}{1 - u} \\ &\quad + \frac{80\pi^2 C A(Q^2)}{\beta_0} \int_0^\infty e^{-ut} R(u, t) \left( \frac{1}{2 - u} - \frac{1}{3 - u} \right) du. \end{aligned} \quad (4.12)$$

As one sees, the structure of the IR renormalon poles is very simple; we encounter only a finite number of single poles located at  $u_0 = 1, 2$  and  $3$ .

In the same manner we get from Eq. (4.11)

$$\begin{aligned}
Q^2 F_{\eta' g^* g^*}^q(Q^2, \omega = 0) &= -\frac{64\pi^2 C(1 + A(Q^2))}{\beta_0} \int_0^\infty du e^{-ut} R(u, t) \frac{1}{(2-u)(3-u)} \\
&+ \frac{640\pi^2 C A(Q^2)}{\beta_0} \int_0^\infty du e^{-ut} R(u, t) \frac{1}{(3-u)(4-u)(5-u)}. \tag{4.13}
\end{aligned}$$

In this case the single IR renormalon poles are located at the points  $u_0 = 2, 3, 4$  and  $5$ .

In order to get the IR renormalon structure of the integrands in Eq. (4.6), we have to expand the hypergeometric function  ${}_2F_1(a, b; c; z)$  in powers of  $z$  (see Eq. (4.3)), where the condition  $|z| < 1$  must hold. But the argument of the function  ${}_2F_1(a, b; c; 2\omega/(1+\omega))$  satisfies this requirement only in the region  $\omega \in (0, 1)$ . In the region  $\omega \in (-1, 0)$  expression (4.4) has to be used, since in this region  $2\omega/(\omega - 1) < 1$ . But regardless of the expansion region, we obtain in both cases the same IR renormalon structure. Adding to this argumentation the evident fact that the vertex function is symmetric under the replacement  $\omega \leftrightarrow -\omega$  (cf. Eq. (2.31)), we can restrict the study of the form factor  $Q^2 F_{\eta' g^* g^*}^q(Q^2, \omega)$  to the region  $\omega \in (0, 1)$ . Then, we can expand the hypergeometric functions  ${}_2F_1(a, b; c; 2\omega/(1+\omega))$  in the region  $\omega \in (0, 1)$ , via Eq. (4.3). For example, for one of these functions, we get

$$\begin{aligned}
B(2, 2-u) {}_2F_1(1, 2; 4-u; \beta) &= \frac{\Gamma(2)\Gamma(2-u)}{\Gamma(4-u)} \sum_{k=0}^{\infty} \frac{(1)_k (2)_k}{(4-u)_k} \frac{\beta^k}{k!} \\
&= \sum_{k=0}^{\infty} \frac{\Gamma(k+2)\Gamma(2-u)}{\Gamma(k+4-u)} \beta^k = \sum_{k=0}^{\infty} B(k+2, 2-u) \beta^k
\end{aligned}$$

with  $\beta$  being equal to  $2\omega/(1+\omega)$ . The remaining terms in Eq. (4.6) can be treated in the same manner and as a result we obtain

$$\begin{aligned}
Q^2 F_{\eta' g^* g^*}^q(Q^2, \omega) &= -\frac{32\pi^2 C[1 + A(Q^2)]}{\beta_0(1+\omega)} \int_0^\infty du e^{-ut} R(u, t) \\
&\times \sum_{k=0}^{\infty} [B(2-u, k+2) + B(2, k+2-u)] \beta^k \\
&+ \frac{160\pi^2 C A(Q^2)}{\beta_0(1+\omega)} \int_0^\infty du e^{-ut} R(u, t) \sum_{k=0}^{\infty} [B(3-u, k+3) + B(3, k+3-u)] \beta^k. \tag{4.14}
\end{aligned}$$

The IR renormalon structure of the integrands in Eq. (4.14) is quite clear now. In fact, we can write the Beta functions entering Eq. (4.14) in the following form

$$B(2, k+2-u) = \frac{\Gamma(2)\Gamma(k+2-u)}{\Gamma(k+4-u)} = \frac{1}{(k+2-u)(k+3-u)},$$

and correspondingly

$$\begin{aligned}
B(2-u, k+2) &= \frac{\Gamma(k+2)}{(2-u)(3-u)\dots(k+3-u)}, \\
B(3, k+3-u) &= \frac{2}{(k+3-u)(k+4-u)(k+5-u)},
\end{aligned}$$

$$B(3-u, k+3) = \frac{\Gamma(k+3)}{(3-u)(4-u)\dots(k+5-u)}.$$

Here we have an infinite number of single IR renormalon poles located at the points  $u_0 = k+2, k+3; u_0 = 2, 3, \dots, k+3; u_0 = k+3, k+4, k+5$  and  $u_0 = 3, 4, \dots, k+5$ , respectively.

The last question to be answered is, whether one can use our results, obtained in the context of the RC method, in the limit  $Q^2 \rightarrow \infty$  in order to regain the asymptotic form of the form factor  $F_{\eta'g^*g^*}^q(Q^2 \rightarrow \infty, \omega)$ . It is clear that regardless of the methods employed and the approximations done in the limit  $Q^2 \rightarrow \infty$ , the form factor  $F_{\eta'g^*g^*}^q(Q^2, \omega)$  must reach its asymptotic form. This is true, of course, for our computations, as we estimate power-suppressed corrections to the form factor  $Q^2 F_{\eta'g^*g^*}^q(Q^2, \omega)$ , which become important in a region of  $Q^2 \sim$  of a few GeV<sup>2</sup>, but vanish in the asymptotic limit. As we have emphasized in Sect. II, in the asymptotic limit the gluon DA of the  $\eta'$ -meson satisfies  $\phi^g(x, Q^2) \rightarrow 0$  and hence

$$Q^2 F_{\eta'g^*g^*}^q(Q^2, \omega) \xrightarrow{Q^2 \rightarrow \infty} 0.$$

The DA of the quark component  $\phi^q(x, Q^2)$  of the  $\eta'$  meson evolves for  $Q^2 \rightarrow \infty$  to the asymptotic DA (2.41) and all non-asymptotic terms in  $\phi^q(x, Q^2)$  proportional to  $C_n^{3/2}(x - \bar{x})$ ,  $n > 0$  (in our case  $\sim A(Q^2)$ ) vanish. Therefore, the results, which we shall obtain here, describe not only the asymptotic limit of  $Q^2 F_{\eta'g^*g^*}^q(Q^2, \omega)$ , but also the asymptotic limit of the vertex function  $Q^2 F_{\eta'g^*g^*}(Q^2, \omega)$  itself.

In the limit  $Q^2 \rightarrow \infty$  the asymmetry parameter can take values  $\omega \rightarrow \pm 1$  (if we pass to the limit  $Q^2 \rightarrow \infty$  at fixed  $Q_2^2$  or  $Q_1^2$ ),  $\omega = 0$  ( $Q_1^2 = Q_2^2$  and  $Q^2 \rightarrow \infty$ ) or  $\omega \neq \pm 1, 0$  (if we take the limit  $Q^2 \rightarrow \infty$  at fixed  $\omega$ ). We consider here all possibilities: a)  $Q^2 \rightarrow \infty, \omega \rightarrow \pm 1$ , b)  $Q^2 \rightarrow \infty, \omega = 0$  and c)  $Q^2 \rightarrow \infty, \omega \neq \pm 1, 0$ . In the limit  $Q^2 \rightarrow \infty$ , we also take into account that the second term in the expansion  $\alpha_s(Q^2 \lambda)$  (3.8) has to be neglected. In other words, in the limit  $Q^2 \rightarrow \infty$ , we find

$$\int_0^\infty e^{-ut} R(u, t) du \rightarrow \int_0^\infty e^{-ut} du. \quad (4.15)$$

We begin from the simpler case a). In Eq. (4.12) we have already obtained the desired limit, but  $A(Q^2) \neq 0$ . Taking into account Eq. (4.15) and  $A(Q^2) \rightarrow 0$ , we get

$$Q^2 F_{\eta'gg^*}(Q^2, \omega = \pm 1) \xrightarrow{Q^2 \rightarrow \infty} -\frac{16\pi^2 C}{\beta_0} \int_0^\infty \frac{e^{-ut} du}{1-u} = -\frac{16\pi^2 C}{\beta_0} \frac{\text{li}(\lambda)}{\lambda}.$$

It is easy to show that using only the leading term in the expansion of  $\text{li}(\lambda)/\lambda$  (see, Eq. (3.15)), we find

$$Q^2 F_{\eta'gg^*}(Q^2, \omega = \pm 1) \xrightarrow{Q^2 \rightarrow \infty} -4\pi C \alpha_s(Q^2). \quad (4.16)$$

The limit  $Q^2 \rightarrow \infty, \omega = 0$  can be analyzed by similar means. Thus, from Eq. (4.13) we get

$$\begin{aligned} Q^2 F_{\eta'g^*g^*}(Q^2, \omega = 0) &\xrightarrow{Q^2 \rightarrow \infty} -\frac{64\pi^2 C}{\beta_0} \int_0^\infty \frac{e^{-ut} du}{(2-u)(3-u)} \\ &= -\frac{64\pi^2 C}{\beta_0} \left[ \frac{\text{li}(\lambda^2)}{\lambda^2} - \frac{\text{li}(\lambda^3)}{\lambda^3} \right], \end{aligned}$$

which in the limit under consideration simplifies to

$$Q^2 F_{\eta' g^* g^*}(Q^2, \omega = 0) \xrightarrow{Q^2 \rightarrow \infty} -\frac{8\pi C \alpha_s(Q^2)}{3}. \quad (4.17)$$

Now let us consider the more interesting case c). Then, from Eqs. (4.6) and (4.15), we obtain

$$\begin{aligned} Q^2 F_{\eta' g^* g^*}(Q^2, \omega) &\xrightarrow{Q^2 \rightarrow \infty} -\frac{32\pi^2 C}{\beta_0(1+\omega)} \int_0^\infty du e^{-ut} B(2, 2-u) \\ &\times \left[ {}_2F_1\left(1, 2; 4-u; \frac{2\omega}{1+\omega}\right) + {}_2F_1\left(1, 2-u; 4-u; \frac{2\omega}{1+\omega}\right) \right]. \end{aligned} \quad (4.18)$$

As an example, we analyze the second term in Eq. (4.18) (see also Eq. (4.14))

$$\begin{aligned} \int_0^\infty du e^{-ut} B(2, 2-u) {}_2F_1(1, 2-u; 4-u; \beta) &= \int_0^\infty du e^{-ut} \sum_{k=0}^\infty B(2, k+2-u) \beta^k \\ &= \sum_{k=0}^\infty \Gamma(2) \beta^k \int_0^\infty du e^{-ut} \left( \frac{1}{k+2-u} - \frac{1}{k+3-u} \right) = \sum_{k=0}^\infty \Gamma(2) \left[ \frac{li(\lambda^{k+2})}{\lambda^{k+2}} - \frac{li(\lambda^{k+3})}{\lambda^{k+3}} \right] \beta^k. \end{aligned}$$

In the considered limit, one finds

$$\frac{li(\lambda^{k+2})}{\lambda^{k+2}} - \frac{li(\lambda^{k+3})}{\lambda^{k+3}} \rightarrow \frac{1}{\ln \lambda} \left( \frac{1}{k+2} - \frac{1}{k+3} \right) = \frac{1}{\ln \lambda} \frac{1}{(k+2)(k+3)}.$$

Then, the result reads

$$\begin{aligned} \sum_{k=0}^\infty \Gamma(2) \left[ \frac{li(\lambda^{k+2})}{\lambda^{k+2}} - \frac{li(\lambda^{k+3})}{\lambda^{k+3}} \right] \beta^k &\rightarrow \frac{1}{\ln \lambda} \sum_{k=0}^\infty \frac{\Gamma(2)}{(k+2)(k+3)} \beta^k \\ &= \frac{1}{\ln \lambda} \sum_{k=0}^\infty B(2, k+2) \beta^k = \frac{1}{\ln \lambda} B(2, 2) {}_2F_1(1, 2; 4; \beta). \end{aligned}$$

The same method can be applied to the first function in Eq. (4.18), but before doing that, it is instructive to employ the transformation (4.5). After performing all these operations, we find

$$\begin{aligned} Q^2 F_{\eta' g^* g^*}(Q^2, \omega) &\xrightarrow{Q^2 \rightarrow \infty} -\frac{64\pi^2 C}{\beta_0(1+\omega)} \frac{1}{\ln \lambda} B(2, 2) {}_2F_1(1, 2; 4; \beta) \\ &= -\frac{8\pi C \alpha_s(Q^2)}{3(1+\omega)} {}_2F_1(1, 2; 4; \beta). \end{aligned} \quad (4.19)$$

Taking into account the expression for the hypergeometric function  ${}_2F_1(1, 2; 4; \beta)$  in terms of elementary ones [59]

$${}_2F_1(1, 2; 4; \beta) = \frac{3}{\beta^3} [\beta(2-\beta) + 2(1-\beta) \ln(1-\beta)], \quad (4.20)$$

we finally obtain

$$Q^2 F_{\eta' g^* g^*}(Q^2, \omega) \xrightarrow{Q^2 \rightarrow \infty} -4\pi C \alpha_s(Q^2) f(\omega), \quad f(\omega) = \frac{1}{\omega^2} \left( 1 + \frac{1-\omega^2}{2\omega} \ln \frac{1-\omega}{1+\omega} \right). \quad (4.21)$$

In our argumentations we have tacitly assumed that  $\omega \in (0, 1)$ . But Eq. (4.21) holds for all values of  $\omega \neq \pm 1, 0$ , which is evident from the equality  $f(\omega) = f(-\omega)$ .

Equations (4.16), (4.17) and (4.21) can be obtained in the standard HSA using the corresponding hard-scattering amplitudes (4.9), (4.10) and (2.21). The analysis carried out so far proves the correctness of the RC method leading to the expected expressions for the form factor  $Q^2 F_{\eta' g^* g^*}(Q^2, \omega)$  at  $Q^2 \rightarrow \infty$  and demonstrating at the same time the consistency of the symmetrization of the hard-scattering amplitudes (2.33), (2.34).

### B. Contribution of the gluon component of the $\eta'$ -meson to the form factor $F_{\eta' g^* g^*}(Q^2, \omega)$

The contribution of the gluon component of the  $\eta'$ -meson to the form factor  $F_{\eta' g^* g^*}(Q^2, \omega)$  can be computed using the methods described in the previous subsection.

Using Eq. (2.34) for the hard-scattering amplitude  $T_1^g(x, Q^2, \omega)$ , the first equality in Eq. (2.30) and the gluon component of the  $\eta'$ -meson DA, we have for the gluon part of the form factor

$$Q^2 F_{\eta' g^* g^*}^g(Q^2, \omega) = \frac{4\pi^2 C B(Q^2)}{3\beta_0} \int_0^\infty du e^{-ut} R(u, t) \left[ \int_0^1 dx x^{1-u} \bar{x}(x - \bar{x}) \frac{(1+\omega)x + (1-\omega)\bar{x}}{\omega[(1+\omega)\bar{x} + (1-\omega)x]} + \int_0^1 dx x \bar{x}^{1-u} (x - \bar{x}) \frac{(1+\omega)x + (1-\omega)\bar{x}}{\omega[(1+\omega)\bar{x} + (1-\omega)x]} \right] \quad (4.22)$$

which after some simple calculations becomes

$$Q^2 F_{\eta' g^* g^*}^g(Q^2, \omega) = \frac{4\pi^2 C B(Q^2)}{3\beta_0 \omega} \int_0^\infty du e^{-ut} R(u, t) \left\{ B(4-u, 2) {}_2F_1(1, 4-u; 6-u; \beta) + B(4, 2-u) {}_2F_1(1, 4; 6-u; \beta) - \frac{2\omega}{1+\omega} B(3, 3-u) [ {}_2F_1(1, 3-u; 6-u; \beta) + {}_2F_1(1, 3; 6-u; \beta) ] - \frac{1-\omega}{1+\omega} [ B(2-u, 4) {}_2F_1(1, 2-u; 6-u; \beta) + B(2, 4-u) {}_2F_1(1, 2; 6-u; \beta) ] \right\}. \quad (4.23)$$

Alternatively, employing the second equality in Eq. (2.30) and corresponding expressions for  $T_2^g(x, Q^2, \omega)$  and  $\phi^g(x, Q^2)$ , we obtain

$$Q^2 F_{\eta' g^* g^*}^g(Q^2, \omega) = -\frac{4\pi^2 C B(Q^2)}{3\beta_0 \omega} \int_0^\infty du e^{-ut} R(u, t) \left\{ B(4-u, 2) {}_2F_1(1, 4-u; 6-u; \tilde{\beta}) + B(4, 2-u) {}_2F_1(1, 4; 6-u; \tilde{\beta}) + \frac{2\omega}{1-\omega} B(3, 3-u) [ {}_2F_1(1, 3-u; 6-u; \tilde{\beta}) + {}_2F_1(1, 3; 6-u; \tilde{\beta}) ] \right\}$$

$$-\frac{1+\omega}{1-\omega} \left[ B(2-u, 4) {}_2F_1(1, 2-u; 6-u; \tilde{\beta}) + B(2, 4-u) {}_2F_1(1, 2; 6-u; \tilde{\beta}) \right] \} . \quad (4.24)$$

In Eqs. (4.23) and (4.24) the  $\beta$  and  $\tilde{\beta}$  are defined as

$$\beta = \frac{2\omega}{1+\omega}, \quad \tilde{\beta} = -\frac{2\omega}{1-\omega}.$$

It is worth noting that Eqs. (4.23) and (4.24) can be obtained from each other by means of the transformation (4.5).

For the  $\eta'$ -meson - on-shell gluon transition, we find

$$Q^2 F_{\eta' gg^*}^g(Q^2, \omega = \pm 1) = \frac{4\pi^2 C B(Q^2)}{3\beta_0} \int_0^\infty du e^{-ut} R(u, t) \times [B(1, 4-u) + B(4, 1-u) - B(2, 3-u) - B(3, 2-u)] , \quad (4.25)$$

or equivalently

$$Q^2 F_{\eta' gg^*}^g(Q^2, \omega = \pm 1) = \frac{4\pi^2 C B(Q^2)}{3\beta_0} \int_0^\infty du e^{-ut} R(u, t) \left( \frac{1}{1-u} - \frac{4}{2-u} + \frac{4}{3-u} \right) . \quad (4.26)$$

In order to obtain Eq. (4.26), it is convenient in the limit  $\omega \rightarrow 1$  to use Eq. (4.23), whereas in the limit  $\omega \rightarrow -1$  Eq. (4.24) has to be used.

The form factor  $Q^2 F_{\eta' g^* g^*}^g(Q^2, \omega = 0)$  can be calculated by employing the following expression for the hard-scattering amplitude

$$T_1^g(x, Q^2, \omega) - T_2^g(x, Q^2, \omega) = \frac{2\pi}{3Q^2} [\alpha_s(Q^2 x) + \alpha_s(Q^2 \bar{x})] \frac{x - \bar{x}}{1 - \omega^2(x - \bar{x})^2} , \quad (4.27)$$

which for  $\omega = 0$  leads to a very simple expression. Then, it is not difficult to demonstrate that

$$Q^2 F_{\eta' g^* g^*}^g(Q^2, \omega = 0) = \frac{16\pi^2 C B(Q^2)}{3\beta_0} \int_0^\infty du e^{-ut} R(u, t) [B(4-u, 2) - 2B(3-u, 3) + B(2-u, 4)] . \quad (4.28)$$

This expression can be recast into the form

$$Q^2 F_{\eta' g^* g^*}^g(Q^2, \omega = 0) = \frac{16\pi^2 C B(Q^2)}{3\beta_0} \int_0^\infty du e^{-ut} R(u, t) \left[ \frac{1}{2-u} - \frac{5}{3-u} + \frac{8}{4-u} - \frac{4}{5-u} \right] . \quad (4.29)$$

The IR renormalon structure of the integrands in Eq. (4.26) and (4.29) is obvious: they have a finite number of IR renormalon poles located at the points  $u_0 = 1, 2, 3$  and  $u_0 = 2, 3, 4, 5$ , respectively. In order to find the IR renormalon structure of the integrand in Eq. (4.23), we expand the corresponding hypergeometric functions over  $\beta = 2\omega/(1+\omega)$  in the region  $\omega \in (0, 1)$ , providing the following result

$$Q^2 F_{\eta' g^* g^*}^g(Q^2, \omega) = \frac{4\pi^2 C B(Q^2)}{3\beta_0 \omega} \int_0^\infty du e^{-ut} R(u, t) \sum_{k=0}^\infty \{ [B(k+4, 2-u)$$

$$\begin{aligned}
& + B(k+4-u, 2)] \beta^k - \frac{1-\omega}{1+\omega} [B(k+2, 4-u) + B(k+2-u, 4)] \beta^k \\
& - [B(k+3, 3-u) + B(k+3-u, 3)] \beta^{k+1} \} . \tag{4.30}
\end{aligned}$$

Using the identities

$$\begin{aligned}
B(k+4, 2-u) &= \frac{\Gamma(k+4)}{(2-u)(3-u)\dots(k+5-u)}, \\
B(k+4-u, 2) &= \frac{1}{(k+4-u)(k+5-u)}, \\
B(k+2, 4-u) &= \frac{\Gamma(k+2)}{(4-u)(5-u)\dots(k+5-u)}, \\
B(k+2-u, 4) &= \frac{6}{(k+2-u)(k+3-u)(k+4-u)(k+5-u)}, \\
B(k+3, 3-u) &= \frac{\Gamma(k+3)}{(3-u)(4-u)\dots(k+5-u)}, \\
B(k+3-u, 3) &= \frac{2}{(k+3-u)(k+4-u)(k+5-u)}
\end{aligned}$$

it is easy to conclude that there is an infinite number of IR renormalon poles being located at the points  $u_0 = 2, 3, \dots, k+5$ ;  $u_0 = k+4, k+5$ ;  $u_0 = 4, 5, \dots, k+5$ ;  $u_0 = k+2, k+3, k+4, k+5$ ;  $u_0 = 3, 4, \dots, k+5$  and  $u_0 = k+3, k+4, k+5$ .

## V. NUMERICAL ANALYSIS

We begin this section by comparing the results obtained within the RC method and IR matching scheme. In Sect. III we have noted that from experimental data only values of nonperturbative parameters  $f_1(2 \text{ GeV})$  and  $f_2(2 \text{ GeV})$  have been extracted. We also know that the lowest-order moment integral and hence the parameter entering our formulas is  $f_2(2 \text{ GeV})$ . Therefore, to make the comparison as clear as possible we should choose the input parameters for the  $\eta'$ -virtual gluon transition in such a way as to determine the behavior of the form factor solely with  $f_2(2 \text{ GeV})$ . This can be easily achieved if we set for the  $\eta'$  meson DA parameters

$$B_2^g(\mu_0^2) = 0, \quad B_2^g(\mu_0^2) = 0.$$

Under such circumstances, the gluon component of the vertex function vanishes. To remove from the analysis the higher-moment integrals  $f_p(Q)$ ,  $p > 2$ , we consider the  $\eta'$ -meson - on-shell gluon transition, i.e., the  $\omega \pm 1$  case. Moreover, we neglect the  $\sim \alpha_S^2$  order term in Eq. (3.2) and set in Eq. (3.8)  $R(u, t) = 1$  because in Eq. (3.19)  $\alpha_s$  is used at the level of the one-loop order accuracy. After these simplifications, the FF is given by the following expression

$$Q^2 F_{\eta' gg^*}(Q^2, \omega = \pm 1) = -\frac{16\pi^2 C}{\beta_0} \int_0^\infty \frac{e^{-ut} du}{1-u} = -4\pi C f_2(Q). \tag{5.1}$$

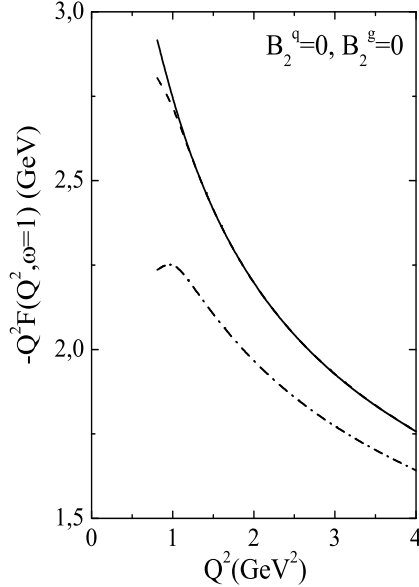


FIG. 3: Scaled  $\eta'g$  transition form factor  $-Q^2 F_{\eta'gg^*}(Q^2, \omega = \pm 1)$  vs.  $Q^2$ . The solid line is computed within the RC method, the dashed one is found using the IR matching scheme with  $f_2(2 \text{ GeV}) \simeq 0.535$ . The dot-dashed curve is obtained in the framework of the IR matching scheme using for  $f_2(2 \text{ GeV})$  the experimental value 0.5.

Results of our computations are shown in Fig. 3, where in order to distinguish the various curves, they are displayed in the region of  $Q^2 \in [0, 4]$ , whereas at higher  $Q^2$  they are close to each other. The RC method and the IR matching scheme<sup>4</sup> lead almost to identical predictions in the entire domain  $1 \text{ GeV}^2 \leq Q^2 \leq 25 \text{ GeV}^2$ , provided that in the IR matching scheme one uses in expression (3.19) the value  $f_2(2 \text{ GeV}) \simeq 0.535$  found within the RC method (3.23). The curve following from the IR matching scheme deviates from prediction obtained with the RC method only for  $Q^2 < 1 \text{ GeV}^2$ . On the other hand, the deviation of that curve, calculated using the experimental value  $f_2(2 \text{ GeV}) \simeq 0.5$ , from the RCM result is sizeable in the region  $Q^2 = 1 \div 2 \text{ GeV}^2$  reaching  $\sim 30\%$  at  $Q^2 = 1 \text{ GeV}^2$ . A similar behavior was observed in the calculation of the pion electromagnetic form factor, carried out within the context of these methods [60]. The difference between the solid and the dot-dashed lines in Fig. 3 is considerably reduced when varying the QCD scale parameter  $\Lambda = 0.3 \text{ GeV}$  or the experimental value of  $f_2(2 \text{ GeV})$  within their corresponding uncertainty domains. But we are not going to make decisive conclusions from these rather model-dependent calculations. Our aim here is to check and demonstrate that the RC method and the IR matching scheme predict in the considered region  $1 \text{ GeV}^2 \leq Q^2 \leq 25 \text{ GeV}^2$  almost identical results that do not contradict experiment.

In order to proceed with the computation of the  $\eta'$ -meson - gluon vertex function and explore the role played by the  $\eta'$  gluon content in this process, we have to define the allowed values of the free input parameters  $B_2^q$  and  $B_2^g$  at the normalization point  $\mu_0$ . These parameters determine the shape of the DA's of the quark and gluon components of the  $\eta'$ -meson and, in general, they have to be extracted from experimental data or computed by non-

<sup>4</sup> Note that in the calculations within the IR matching scheme, Eq. (3.19) with  $N = 4$  has been used.

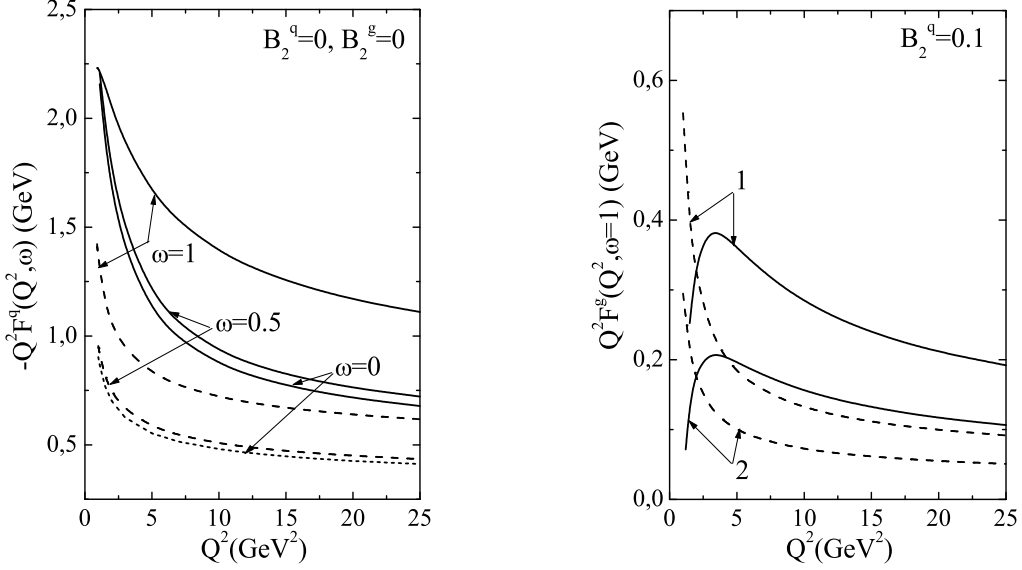


FIG. 4: The quark (left panel) and gluon (right panel) components of the transition form factor  $Q^2 F_{\eta' g^* g^*}^q(Q^2, \omega)$  as functions of  $Q^2$ . The solid curves are obtained using the RC method, whereas the broken lines are calculated within the standard HSA. The quark component is computed at various  $\omega$  values by employing the asymptotic DA. In the right panel correspondence between the curves and the input parameter  $B_2^g$  is for the curves labelled 1:  $B_2^g = 8$ ; and for those labelled 2:  $B_2^g = 4$ .

perturbative techniques. The comparison of the  $\eta'$ -meson-photon electromagnetic transition FF with the corresponding CLEO data led to the conclusion that the  $\eta'$  meson DA must be close to its asymptotic form with the coefficient  $B_2^q \simeq 0.1$  [6] being deduced. This conclusion was made by neglecting the contribution of the gluon component of the  $\eta'$ -meson to the  $\eta' \gamma$  transition FF and, in reality, only the DA of the quark content of the  $\eta'$  was explored. Hence, the  $\eta' \gamma$  transition restricts the combination  $|B_2^g \rho_2^g| < 0.1$  that allows one to keep the DA  $\phi^q(x, Q^2)$  close to its asymptotic form. In this work we choose the parameter  $B_2^g > 0$  and in the region  $B_2^g \in [0, 8]$ . The value  $B_2^q = 0.1$  is already fixed from CLEO data [6].

It is evident that the non-asymptotic terms in the quark and gluon DA's of the  $\eta'$ -meson proportional to  $A(Q^2)$  and  $B(Q^2)$ , respectively, affect the asymptotic value of the  $\eta'$ -meson-gluon transition form factor. Therefore, before presenting contributions from these terms, it is instructive to study the asymptotic FF itself. In the left panel of the Fig. 4 we depict the  $\eta'$ -meson - virtual gluon transition FF as a function of the gluon virtuality  $Q^2$ . For the asymptotic DA the quark component of the form factor coincides with the full one. In the same figure the prediction obtained within the standard HSA are also shown. One sees that in the domain  $1 \text{ GeV}^2 \leq Q^2 \leq 25 \text{ GeV}^2$  the ordinary PQCD results get enhanced by approximately a factor of two due to power corrections. A similar conclusion is valid also for the gluon component of the form factor (right panel in Fig. 4, computed employing the  $\eta'$ -meson DA's).

Here some comments concerning the accuracy of the numerical computations are in order. In Fig. 4 (left panel) and the following ones, the curves obtained within the RC method, as a rule, require a summation of an infinite series. In real numerical computations we truncate

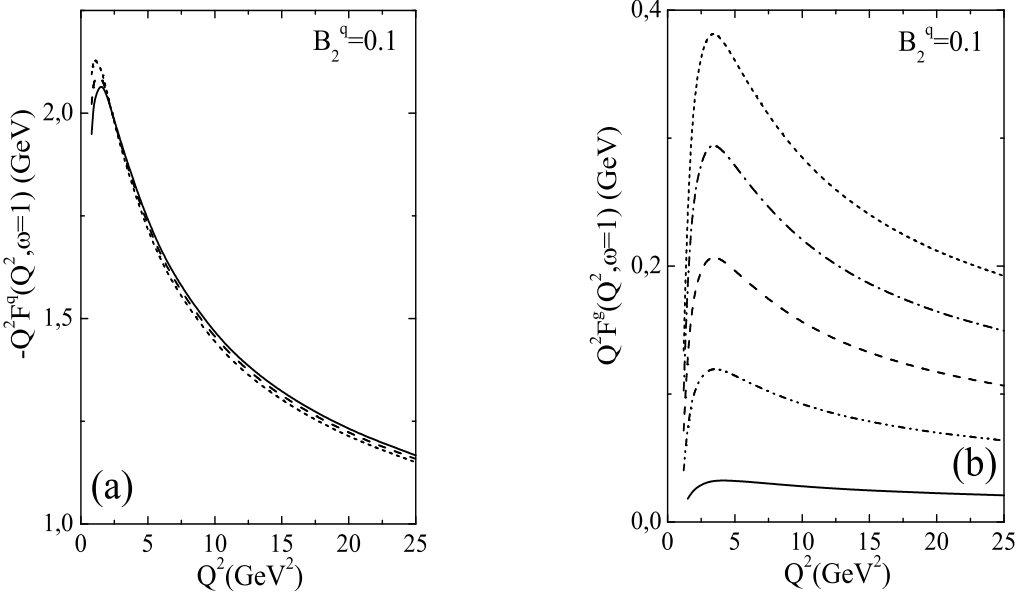


FIG. 5: The contribution of the quark a) and gluon b) components of the  $\eta'$ -meson to the form factor  $Q^2 F_{\eta' gg^*}(Q^2, \omega = \pm 1)$  vs.  $Q^2$ . All curves are obtained in the context of the RC method. The correspondence between all displayed curves and the parameter  $B_2^g$  is:  $B_2^g = 0$  for solid curves;  $B_2^g = 2$  for the dot-dot-dashed curve;  $B_2^g = 4$  for the dashed lines;  $B_2^g = 6$  for the dot-dashed line, and  $B_2^g = 8$  for the short-dashed curves. In figure a) curves corresponding only to  $B_2^g = 0, 4$  and  $8$  are shown.

such a series at some  $k = K_{max}$ . Naturally, the question arises about the convergence rate of this series. Let us explain this problem by considering Fig. 4 as an example. The solid curve with  $\omega = 0.5$  in Fig. 4 (left panel) has been found within the RC method by employing Eq. (4.14). This expression contains series with factorially growing coefficients. For definiteness we analyze the term

$$\begin{aligned} & \int_0^\infty du e^{-ut} R(u, t) \sum_{k=0}^\infty B(k+2, 2-u) \beta^k \\ &= \sum_{k=0}^\infty \int_0^\infty du e^{-ut} R(u, t) \frac{\Gamma(k+2)}{(2-u)(3-u)\dots(k+3-u)} \beta^k. \end{aligned} \quad (5.2)$$

The expansion parameter  $\beta = 2\omega/(1+\omega)$  in Eq. (5.2) at the point  $\omega = 0.9$  is equal to  $\beta = 0.947$ . Below, we write down the values of the Gamma function  $\Gamma(k+2) = (k+1)!$  and the product of  $\beta^k$  with the principal value of the integral

$$I(k) = \int_0^\infty du e^{-ut} R(u, t) \frac{\beta^k}{(2-u)(3-u)\dots(k+3-u)} \quad (5.3)$$

for  $k = 0, 5, 10$  and  $15$

$$\Gamma(2) = 1, \quad \Gamma(7) = 720, \quad \Gamma(12) = 3.99168 \cdot 10^7, \quad \Gamma(17) = 2.0922789888 \cdot 10^{13}$$

and

$$I(0) \simeq 0.11654, \quad I(5) \simeq 1.8044 \cdot 10^{-5},$$

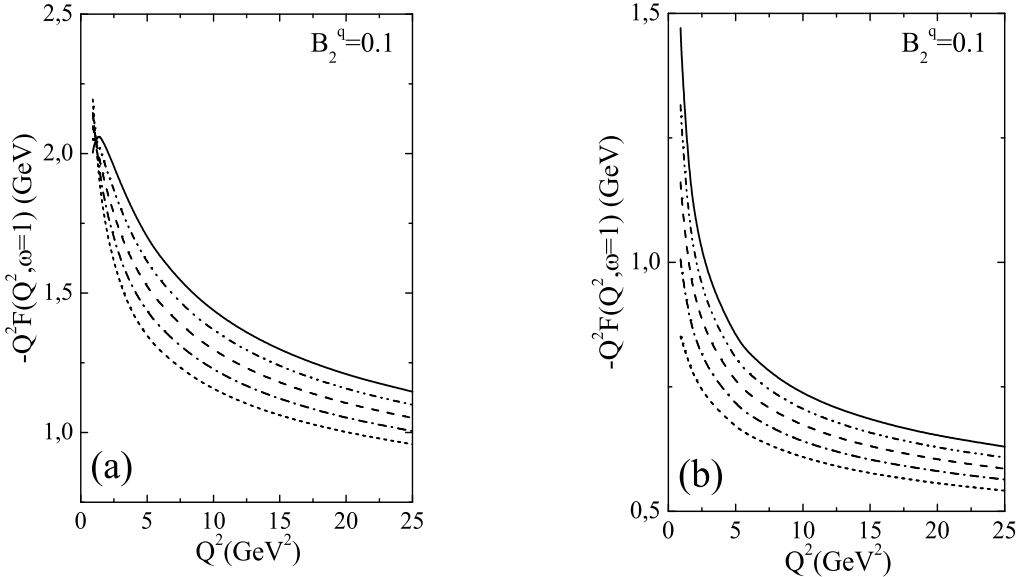


FIG. 6: The form factor  $-Q^2 F_{\eta' gg^*}(Q^2, \omega = \pm 1)$  computed using the RC method a), and the standard HSA b). The correspondence between curves and the parameter  $B_2^g$  is the same as in Fig. 5.

$$I(10) \simeq 6.51583 \cdot 10^{-11} \quad I(15) \simeq 1.54955 \cdot 10^{-17}.$$

As a result, the corresponding terms in the sum given by Eq. (5.2) take the values

$$0.11654, \quad 1.2992 \cdot 10^{-2}, \quad 2.6009 \cdot 10^{-3}, \quad 3.2421 \cdot 10^{-4},$$

respectively. One observes that the convergence rates of the numerical series are high and that we can therefore truncate them, as a rule, at  $K_{max} = 20$ .

We have analysed the impact of the various DA's of the  $\eta'$ -meson on the  $\eta'g$  transition form factor. The quark component of the FF is stable for different values of  $B_2^g \in [0, 8]$ . It is difficult to distinguish corresponding curves and therefore in Fig. 5a we can only plot some of them. In contrast, the gluon component of the form factor demonstrates a rapid growth with  $B_2^g$  (Fig. 5b). As a result, due to different signs of the quark and gluon components of the space-like vertex function, the total vertex function  $Q^2 F_{\eta' gg^*}(Q^2, \omega = \pm 1)$  for  $B_2^g \neq 0$  lies below the asymptotic one (Fig. 6a). Comparing the predictions derived within the RC method with those following from the standard HSA (Fig. 6b), we see a quantitative difference between corresponding curves.

The dependence of the quark and gluon components of the form factor on the asymmetry parameter  $\omega$  at fixed  $Q^2$  and for various DA's of the  $\eta'$ -meson are shown in Fig. 7. Because  $F_{\eta' g^* g^*}(Q^2, \omega)$  is symmetric under the exchange  $\omega \leftrightarrow -\omega$ , we present our results in the region  $0 \leq \omega \leq 1$  only. We have just demonstrated in Fig. 5 that the quark component of the FF  $F_{\eta' gg^*}^q(Q^2, \omega = \pm 1)$  is not sensitive to the use of various  $\eta'$ -meson DA's, employed in our calculations. This is valid also for its behavior as a function of  $\omega$  (Fig. 7a). In accordance with our computations, an effect of the chosen parameter  $B_2^g$  on the gluon component of the FF is considerable in the whole range of  $\omega \in [0, 1]$ .

The magnitude of the quark and gluon components of the form factor for a given DA depends on the total gluon virtuality  $Q^2$  (Fig. 8). In this case both the quark and gluon

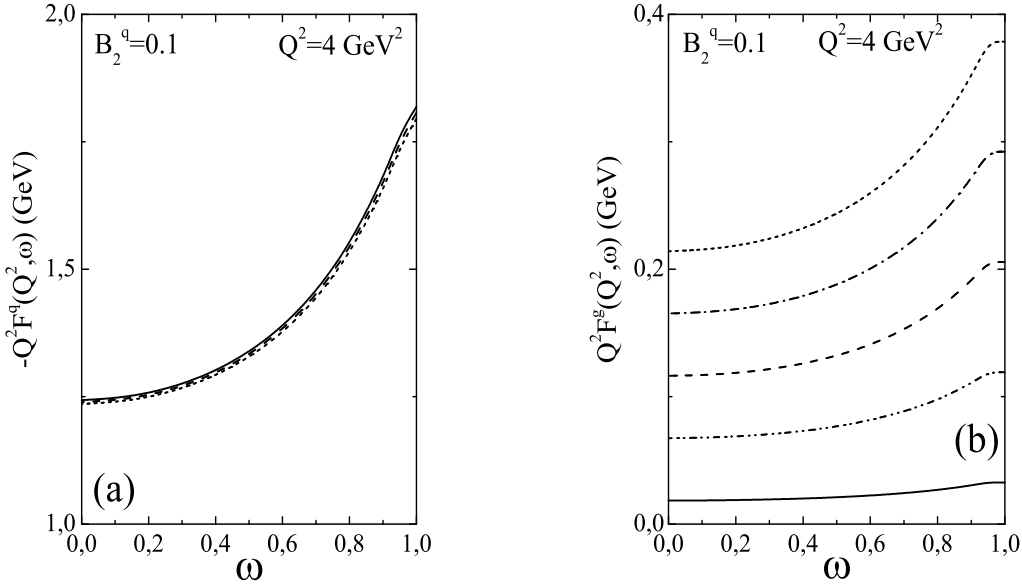


FIG. 7: The quark a) and gluon b) components of the FF at fixed total gluon virtuality  $Q^2 = 4 \text{ GeV}^2$  as functions of the asymmetry parameter  $\omega$ . The RC method is employed. The correspondence between depicted lines and the parameter  $B_2^g$  is the same as in Fig. 5.

contributions to the FF demonstrate sensitivity to the fixed value of  $Q^2$ .

The features of the quark and gluon components of the  $\eta'g^*$  transition FF described above determine the behavior of their sum as a function of the asymmetry parameter  $\omega$  and we get the picture shown in Fig. 9a. Owing to the gluon component, the form factor  $F_{\eta'g^*g^*}(Q^2, \omega)$  depends on the  $\eta'$ -meson DA used in the calculations. For comparison, in Fig. 9b the curves found within the standard HSA are also shown. An enhancement of about a factor of two of the vertex function due to power corrections is evident.

The  $\eta'g^*$  transition FF as function of the first gluon virtuality  $Q_1^2$  at various fixed values of the second one  $Q_2^2$  and for different DA's is plotted in Fig. 10.

## VI. CONCLUDING REMARKS

In this paper we have evaluated power-suppressed corrections  $\sim 1/Q^{2n}$ ,  $n = 1, 2 \dots$  to the space-like  $\eta'$ -meson-virtual gluon transition form factor  $Q^2 F_{\eta'g^*g^*}(Q^2, \omega)$ . To this end, we have employed the standard hard scattering approach and the running coupling method in conjunction with the infrared renormalon calculus. In the calculations, both the quark and the gluon distribution amplitudes of the  $\eta'$  meson have been taken into account. In these model DA's only the first non-asymptotic terms have been retained and the values of the input coefficients  $B_2^q(\mu_0^2)$  and  $B_2^g(\mu_0^2)$  have been estimated using the CLEO data on the  $\eta'\gamma$  electromagnetic transition form factor.

In order to apply the RC method to the considered process, the hard-scattering amplitudes of the corresponding subprocesses have been generalized in such a way as to preserve the symmetry properties of both the hard-scattering amplitudes and the transition form factor itself under the replacements  $x \leftrightarrow \bar{x}$  and  $\omega \leftrightarrow -\omega$ . In the computations within the RC method the Laplace transformed expression for the running coupling has been employed.

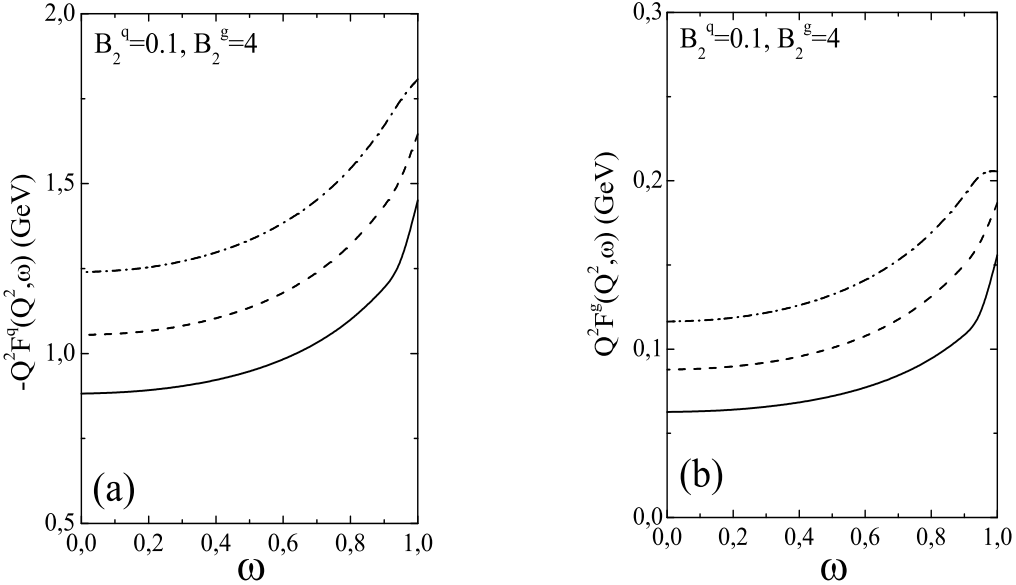


FIG. 8: The quark a) and gluon b) components of the form factor  $Q^2 F_{\eta' g^* g^*}(Q^2, \omega)$  at fixed  $Q^2$  vs.  $\omega$ . The RC method is used. For the solid curves  $Q^2 = 10 \text{ GeV}^2$ , for the dashed ones  $Q^2 = 6 \text{ GeV}^2$ , and for the dot-dashed curves  $Q^2 = 4 \text{ GeV}^2$ .

The Borel resummed form factors obtained this way, have been regularized by means of the principal value prescription. Various limits of the general expression  $Q^2 F_{\eta' g^* g^*}(Q^2, \omega)$  have been found.

Our numerical analysis proves that power corrections considerably enhance the ordinary PQCD predictions for the form factor in the explored region  $1 \text{ GeV}^2 \leq Q^2 \leq 25 \text{ GeV}^2$ . Our investigations also demonstrate that the quark component of the form factor at fixed  $B_2^q = 0.1$  is practically stable for several values of  $B_2^g = 0, 2, 4, 6, 8$ . Contrary to this, the gluon component of the FF is sensitive to the adopted value of  $B_2^g$ . As a consequence, the  $\eta' g^*$  transition FF depends on the gluonic content of the  $\eta'$  meson; in the considered region the gluon contribution reduces the absolute value of the space-like form factor  $Q^2 F_{\eta' g^* g^*}(Q^2, \omega)$ .

The  $\eta' g^*$  transition is a key component of recently proposed mechanisms to account for the CLEO data on B meson exclusive and semi-inclusive  $B \rightarrow \eta' K$  and  $B \rightarrow \eta' X_s$  decays, respectively, and may be useful in studying also other processes. In this paper we have demonstrated that power corrections properly taken into account lead to an enhancement of the  $\eta' g^*$  transition FF. This effect can improve the agreement of the Standard Model predictions for these processes with experimental data.

## Acknowledgments

One of the authors (S.S.A.) would like to thank Prof. S. Randjbar-Daemi and the High Energy Section members for their hospitality in the Abdus Salam ICTP, where this work started and Prof. K. Goeke and the members of the Institute for Theoretical Physics II, where this investigation was completed. Both of us wish to thank A. Bakulev, A. Belitsky, and K. Passek for useful comments. The financial support by DAAD (S.S.A.) is gratefully acknowledged.

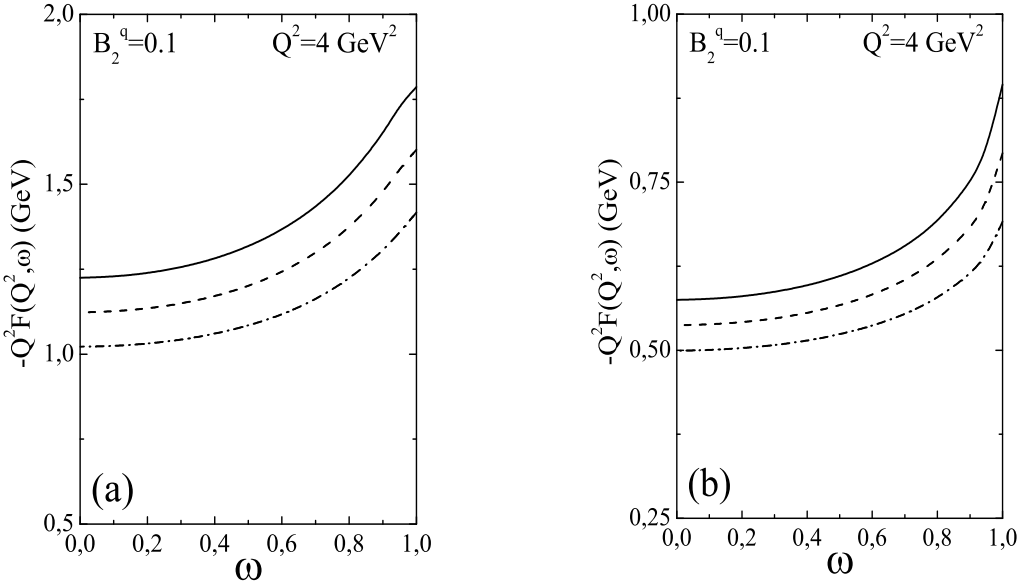


FIG. 9: The FF  $-Q^2 F_{\eta' g^* g^*}(Q^2, \omega)$  obtained employing the RC method a) and the standard HSA b) as functions of  $\omega$ . For the solid lines  $B_2^g = 0$ , for the dashed lines  $B_2^g = 4$  and for the dot-dashed lines  $B_2^g = 8$ .

- 
- [1] CLEO Collaboration, J. Gronberg et al., Phys. Rev. D 57, 33 (1998) [hep-ex/9707031].  
 [2] CLEO Collaboration, B. H. Behrens et al., Phys. Rev. Lett. 80, 3710 (1998) [hep-ex/9801012];  
 T. E. Browder et al., Phys. Rev. Lett. 81, 1786 (1998) [hep-ex/9804018].  
 [3] J. Cao, F.-G. Cao, T. Huang, and B.-Q. Ma, Phys. Rev. D 58, 113006 (1998) [hep-ph/9807508].  
 [4] R. Jakob, P. Kroll, and M. Raulfs, J. Phys. G 22, 45 (1996) [hep-ph/9410304].  
 [5] Th. Feldmann and P. Kroll, Eur. Phys. J. C 5, 327 (1998) [hep-ph/9711231].  
 [6] S. S. Agaev, Phys. Rev. D 64, 014007 (2001).  
 [7] M. K. Chase, Nucl. Phys. B 174, 109 (1980).  
 [8] M. V. Terentev, Sov. J. Nucl. Phys. 33, 911 (1981) [Yad. Fiz. 33, 1692 (1981)].  
 [9] T. Ohrndorf, Nucl. Phys. B 186, 153 (1981).  
 [10] M. A. Shifman and M. I. Vysotsky, Nucl. Phys. B 186, 475 (1981).  
 [11] V. N. Baier and A. G. Grozin, Nucl. Phys. B 192, 476 (1981).  
 [12] D. Atwood and A. Soni, Phys. Lett. B 405, 150 (1997) [hep-ph/9704357].  
 [13] W.-S. Hou and B. Tseng, Phys. Rev. Lett. 80, 434 (1998) [hep-ph/9705304].  
 [14] A. L. Kagan and A. A. Petrov, hep-ph/9707354.  
 [15] M. Ahmady, E. Kou, and A. Sugamoto, Phys. Rev. D 58, 014015 (1998) [hep-ph/9710509].  
 [16] A. Ali, J. Chay, C. Greub, and P. Ko, Phys. Lett. B 424, 161 (1998) [hep-ph/9712372]; D. Du, C. S. Kim and Y. Yang, Phys Lett. B 426, 133 (1998) [hep-ph/9711428].  
 [17] I. Halperin and A. Zhitnitsky, Phys. Rev. D 56, 7247 (1997) [hep-ph/9704412]; Phys. Rev. Lett. 80, 438 (1998) [hep-ph/9705251].  
 [18] M. Franz, P. V. Pobylitsa, M. V. Polyakov, and K. Goeke, Phys. Lett. B 454, 335 (1999) [hep-ph/9810343]; M. Franz, M. V. Polyakov and K. Goeke, Phys. Rev. D 62, 074024 (2000)

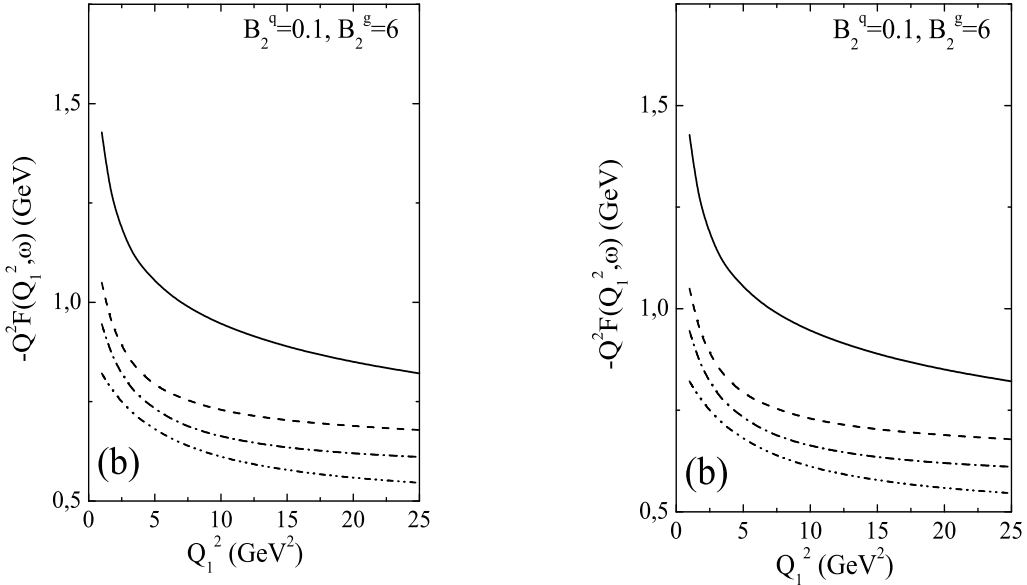


FIG. 10: The form factor  $-Q^2 F_{\eta' g^* g^*}(Q_1^2, \omega)$  at different fixed values of  $Q_1^2$ . For the solid curves  $Q_2^2 = 1 \text{ GeV}^2$ , for the dashed curves  $Q_2^2 = 5 \text{ GeV}^2$ , for the dot-dashed curves  $Q_2^2 = 10 \text{ GeV}^2$ , and for the dot-dot-dashed curves  $Q_2^2 = 25 \text{ GeV}^2$ .

[hep-ph/0002240].

- [19] A. S. Dighe, M. Gronau, and J. Rosner, Phys. Lett. B 367, 357 (1996) [Erratum-ibid. B 377, 325 (1996)] [hep-ph/9509428]; H. Fritzsch, Phys. Lett. B 415, 83, (1997) [hep-ph/9708348]; A. Datta, X.-G. He, and S. Pakvasa, Phys. Lett. B 419, 369 (1998) [hep-ph/9707259]; X.-G. He and G.-L. Lin, Phys. Lett. B 454, 123 (1999) [hep-ph/9809204].
- [20] J. O. Eeg, A. Hiorth, and A. D. Polosa, Phys. Rev. D 65, 054030 (2002) [hep-ph/0109201]; E. Kou and A. I. Sanda, Phys. Lett. B 525, 240 (2002) [hep-ph/0106159]; A. Deandrea and A. D. Polosa, Eur. Phys. J. C 22, 677 (2002) [hep-ph/0107234].
- [21] T. Muta and M.-Z. Yang, Phys. Rev. D 61, 054007 (2000) [hep-ph/9909484].
- [22] M.-Z. Yang and Y.-D. Yang, Nucl. Phys. B 609, 469 (2001) [hep-ph/0012208].
- [23] A. Ali and A. Ya. Parkhomenko, Phys. Rev. D 65, 074020 (2002) [hep-ph/0012212].
- [24] P. Kroll and K. Passek-Kumerički, hep-ph/0210045.
- [25] G. P. Lepage and S. J. Brodsky, Phys. Rev. D 22, 2157 (1980); A. V. Efremov and A. V. Radyushkin, Phys. Lett. B 94, 245 (1980); Theor. Mat. Phys. 42, 97 (1980) [Teor. Mat. Fiz. **42**, 147 (1980)] A. Duncan and A. H. Mueller, Phys. Rev. D 21, 1636 (1980).
- [26] M. Beneke, Phys. Rep. 317, 1 (1999) [hep-ph/9807443].
- [27] S. J. Brodsky, G. P. Lepage, and P. B. Mackenzie, Phys. Rev. D 25, 228 (1983).
- [28] S. S. Agaev, Phys. Lett. B 360, 117 (1995) [Erratum-ibid. B 369 (1996) 379]. Mod. Phys. Lett. A 10, 2009 (1995); ibid. A 11, 957 (1996); ibid. A 13, 2637 (1998) [hep-ph/9805278].
- [29] S. S. Agaev, A. I. Mukhtarov, and Y. V. Mamedova, Mod. Phys. Lett. A 15, 1419 (2000).
- [30] P. Gosdzinsky and N. Kivel, Nucl. Phys. B 521, 274 (1998) [hep-ph/9707367]; S. S. Agaev and A. I. Mukhtarov, Int. J. Mod. Phys. A 16, 3179 (2001).
- [31] D. V. Shirkov and I. L. Solovtsov, Phys. Rev. Lett. 79, 1209 (1997) [hep-ph/9704333].
- [32] A. I. Karanikas and N. G. Stefanis, Phys. Lett. B 504, 225 (2001) [hep-ph/0101031].
- [33] N. G. Stefanis, in 8th Adriatic Meeting and Central European Symposia on Particle Physics

in the New Millennium, Dubrovnik, Croatia, 4-14 Sep 2001 to appear in Lect. Notes Phys. by Springer Verlag [hep-ph/0203103].

- [34] A. Petrov, Phys. Rev. D 58, 054004 (1998) [hep-ph/9712497].
- [35] J. L. Rosner, Phys. Rev. D 27, 1101 (1983).
- [36] E. Kou, Phys. Rev. D 63, 054027 (2001) [hep-ph/9908214].
- [37] KLOE Collaboration, A. Aloisio et al., Phys. Lett. B 541, 45 (2002) [hep-ex/0206010].
- [38] Th. Feldmann, P. Kroll, and B. Stech, Phys. Lett. B 449, 339 (1999) [hep-ph/9812269].
- [39] Th. Feldmann, P. Kroll and B. Stech, Phys. Rev. D 58, 114006 (1998) [hep-ph/9802409].
- [40] H. Leutwyler, Nucl. Phys. (Proc. Suppl.) 64, 223 (1998) [hep-ph/9709408]; R. Kaiser and H. Leutwyler, [hep-ph/9806336].
- [41] Th. Feldmann, Int. J. Mod. Phys. A 15, 159 (2000) [hep-ph/9907491].
- [42] N. G. Stefanis, W. Schroers, and H. C. Kim, Eur. Phys. J. C 18, 137 (2000) [hep-ph/0005218].
- [43] R. D. Field, R. Gupta, S. Otto, and L. Chang, Nucl. Phys. B 186, 429 (1981).
- [44] F.-M. Dittes and A. V. Radyushkin, Sov. J. Nucl. Phys. 34, 293 (1981) [Yad. Fiz. 34, 529 (1981)]; E. Braaten and S.-M. Tse, Phys. Rev. D 35, 2255 (1987).
- [45] F. del Aguila and M. K. Chase, Nucl. Phys. B 193, 517 (1981); E. Braaten, Phys. Rev. D 28, 524 (1983); E. P. Kadantseva, S. V. Mikhailov, and A. V. Radyushkin, Sov. J. Nucl. Phys. 44, 326 (1986) [Yad. Fiz. 44, 507 (1986)]; B. Nižić, Phys. Rev. D 35, 80 (1987); B. Melić, B. Nižić, and K. Passek, Phys. Rev. D 65, 053020 (2002) [hep-ph/0107295].
- [46] A. P. Bakulev, S. V. Mikhailov and N. G. Stefanis, Phys. Lett. B 508, 279 (2001) [hep-ph/0103119]; hep-ph/0104290; hep-ph/0212250.
- [47] A. V. Belitsky and D. Müller, Nucl. Phys. B 537, 397 (1999) [hep-ph/9804379].
- [48] H. Bateman and A. Erdélyi, Higher Transcendental Functions (McGraw-Hill, New York, 1953), Vol. 2.
- [49] H. Contopanagos and G. Sterman, Nucl. Phys. B 419, 77 (1994) [hep-ph/9310313].
- [50] G. 't Hooft, in The Whys of Subnuclear Physics, Proceedings of the International School, Erice, 1977, edited by A. Zichichi (Plenum, New York, 1978); V. I. Zakharov, Nucl. Phys. B 385, 452 (1992).
- [51] H. Bateman and A. Erdélyi, Tables of Integral Transforms (McGraw-Hill, New York, 1954), Vol. 1.
- [52] B. R. Webber, JHEP 9810, 012 (1998) [hep-ph/9805484].
- [53] M. Dasgupta and G. P. Salam, JHEP 0208 (2002) 032 [hep-ph/0208073].
- [54] P. A. Movilla Fernández, S. Bethke, O. Biebel, S. Kluth, Eur. Phys. J. C 22, 1 (2001) [hep-ex/0105059].
- [55] H1 Collaboration, C. Adloff et al., Eur. Phys. J. C 14, 255 (2000); [Erratum-ibid. C 18, 417 (2000)] [hep-ex/9912052].
- [56] New Muon Collaboration, M. Arneodo et al., Nucl. Phys. B 483, 3 (1997); CCFR/NuTeV Collaboration, W. G. Seligman et al., Phys. Rev. Lett. 79, 1213 (1997); M. Virchaux and A. Milsztajn, Phys. Lett. B 274, 221 (1992); A. L. Kataev, A. V. Kotikov, G. Parente, and A. V. Sidorov, Phys. Lett. B 417, 374 (1998) [hep-ph/9706534].
- [57] M. Dasgupta and B. R. Webber, Phys. Lett. B 382, 273 (1996) [hep-ph/9604388]; Nucl. Phys. B 484, 247 (1997) [hep-ph/9608394].
- [58] A. P. Prudnikov, Yu. A. Brychkov, and O. I. Marichev, Integrals and Series, Vol. 1: Elementary Functions (Gordon and Breach, New York, 1986).
- [59] A. P. Prudnikov, Yu. A. Brychkov, and O. I. Marichev, Integrals and Series, Vol. 3: More Special Functions (Gordon and Breach, New York, 1990).

- [60] S. S. Agaev, Nucl. Phys. B (Proc. Suppl.) 74, 155 (1999) [hep-ph/9807444].